CHALMERS

Crane foundations on soft soil

An analysis of conservatism in bearing capacity predictions

Master's Thesis in the Master's Programme Infrastructure and Environmental Engineering

ERIK LUNDBLAD
KIM PLATH

Department of Civil and Environmental Engineering
Division of Geology and Geotechnics
Engineering Geology and Geotechnics Research Group
CHALMERS UNIVERSITY OF TECHNOLOGY
Master's Thesis BOMX02-17-13
Gothenburg, Sweden 2017

MASTER'S THESIS BOMX02-17-13

Crane foundations on soft soil

An analysis of conservatism in bearing capacity predictions

Master's Thesis in the Master's Programme
Infrastructure and Environmental Engineering

ERIK LUNDBLAD
KIM PLATH

Department of Civil and Environmental Engineering
Division of Geology and Geotechnics
Engineering Geology and Geotechnics Research Group
CHALMERS UNIVERSITY OF TECHNOLOGY
Göteborg, Sweden 2017

Crane foundations on soft soil
An analysis of conservatism in bearing capacity predictions

Master's Thesis in the Master's Programme
Infrastructure and Environmental Engineering

ERIK LUNDBLAD

KIM PLATH

© ERIK LUNDBLAD, KIM PLATH, 2017

Examensarbete BOMX02-17-13 / Institutionen för bygg- och miljöteknik,
Chalmers tekniska högskola 2017

Department of Civil and Environmental Engineering
Division of Geology and Geotechnics
Engineering Geology and Geotechnics Research Group
Chalmers University of Technology
SE-412 96 Göteborg
Sweden
Telephone: +46 (0)31-772 10 00

Cover:
Junttan PM 23 LC, © Junttan
Department of Civil and Environmental Engineering
Göteborg, Sweden, 2017

Crane foundations on soft soil

An analysis of conservatism in bearing capacity predictions

Master's Thesis in the Master's Programme Infrastructure and Environmental Engineering

ERIK LUNDBLAD
KIM PLATH
Department of Civil and Environmental Engineering
Division of Geology and Geotechnics
Engineering Geology and Geotechnics Research Group
Chalmers University of Technology

ABSTRACT

Cranes are used for piling and lifting and are therefore an essential part of the construction industry. Heavy machines coupled with poor ground conditions can however cause ground failures with machine damages and personal injuries as a consequence. In Sweden there is a lack of industry guidelines concerning the handling of heavy machines on soft soil and proper dimensioning is not always done. Dimensioning of crane foundations and working platforms is usually performed analytically with the general bearing capacity equation. This formula is believed to be too conservative in the case of a working platform overlying soft soil. In this study, finite-element modelling was performed in PLAXIS to evaluate whether the general bearing capacity equation can be used to properly model crane foundations on working platforms of fill overlying soft clay. A Mohr-Coulomb model was used for a hypothetical case resembling the same conditions as for the analytical formula. A NGI-ADP model was then used for a realistic case with soil parameters representing Gothenburg clay. Here, the effects on bearing capacity caused by shear strength anisotropy of clay and the increase in shear strength with depth were studied. For the hypothetical cases studied, the results showed that the analytical solution is similar to the finite-element solution for an isotropic soft clay. Hence, the general bearing capacity equation can be used to properly model crane foundations on working platforms overlying an isotropic soft clay. Incorporating anisotropic shear strength and shear strength that increased linearly with depth lead to an increased bearing capacity and resulted in less required fill. The general bearing capacity equation can therefore be conservative if an anisotropic and nonhomogeneous shear strength profile is identified in the soil. Furthermore, simulations with a low fill thickness showed local shear failure, while thicker fills resulted in a punching shear failure. The failure mechanism, however, was very shallow and only the shear strength in the top of the clay was of importance for the bearing capacity. The shear strength and stiffness of the entire soil profile is however still of importance to account for settlements; especially for thicker working platforms.

Key words: Geotechnics, Soft clay, Working platform, Crane foundations, Bearing capacity, PLAXIS

Kranfundament på lös jord

En analys av konservatism i förutsägelser av bärighetskapacitet

Examensarbete inom mastersprogrammet Infrastructure and Environmental Engineering

ERIK LUNDBLAD
KIM PLATH
Institutionen för bygg- och miljöteknik
Avdelningen för geologi och geoteknik
Forskargruppen för geologi och geoteknik
Chalmers tekniska högskola

SAMMANFATTNING

Kranar används för pålning och tunga lyft och är därmed essentiella inom byggbranschen. Tunga maskiner i kombination med dåliga markförhållanden kan dock resultera i markbrott, med maskin- och personskador som konsekvens. I Sverige råder brist på branschriktlinjer gällande hanteringen av tunga maskiner på lös jord vilket kan leda till att dimensionering inte görs ordentligt. Dimensionering av kranfundament och arbetsbäddar utförs vanligtvis analytiskt med hjälp av den allmänna bärighetsekvationen. Ekvationen antas vara konservativ när geostrukturen består av en arbetsbädd av fyllnadsmaterial på lös lera. I den här avhandlingen användes finita-element-modellering med mjukvaran PLAXIS för att utvärdera om den allmänna bärighetsekvationen beaktar kranfundament på fyllnadsmaterial över lös lera på ett korrekt sätt. En Mohr-Coulomb modell användes för ett hypotetiskt fall, med liknande förutsättningar som för den allmänna bärighetsekvationen. Därefter användes en NGI-ADP modell för ett verklighetstroget fall med jordparametrar som motsvarar Göteborgslera. Här studerades effekten av lerans anisotropi och ökning av skjuvhållfasthet med djupet. För de hypotetiska fallen som studerades visade resultatet att den analytiska lösningen var snarlik den finita-element-lösningen för en homogen lera. Därmed är den allmänna bärighetsekvationen en bra metod för att dimensionera kranfundament när geostrukturen består av en arbetsbädd på lös, homogen lera. Implementeringen av anisotropisk skjuvhållfasthet och skjuvhållfasthet som ökade linjärt med djupet ledde till en ökad bärighetskapacitet och resulterade i mindre fyllnadstjocklek. Den allmänna bärighetsekvationen kan därmed vara konservativ om ett anisotropiskt och inhomogent beteende identifieras i jorden. Vidare visade simuleringar med en låg fyllnadtjocklek ett lokalt skjuvbrott, medan tjockare fyllnadstjocklek resulterade i stansningsbrott. Brottmekansimen var dock väldigt grund och endast skjuvhållfastheten i toppen av leran var av betydelse för bärighetskapaciten. Skjuvhållfastheten och styvheten för hela jordprofilen är dock fortfarande av betydelse för att beakta sättningar; speciellt för geostrukturer bestående av tjockare arbetsbäddar.

Nyckelord: Geoteknik, Lös lera, Arbetsbädd, Kranfundament, Bärighetskapacitet, PLAXIS

Contents

Figures

Tables

Preface

This Thesis was written from January 2017 to June 2017 as part of the Master's programme Infrastructure and Environmental Engineering at Chalmers University of Technology. The topic was initiated by the company ELU, who we want to thank for providing us office space, literature and knowledge. We are especially grateful towards the geotechnical division consisting of Lars Hall, Mehras Shahrestanakizadeh and Therese Hedman for their help and support. We would also like to thank Jelke Dijkstra, our supervisor and examiner at Chalmers, who assisted us with our work. The discussions we had and the input we received was greatly appreciated.

Gothenburg June 2017

Erik Lundblad
Kim Plath

Notations

Roman letters

c	Cohesion
c'	Cohesion intercept
d	Friction layer depth, thickness of working platform
E	Young's modulus
E_{oed}	Oedometer modulus
G	Shear modulus
G_{ur}	Unloading/reloading shear modulus
K	Bulk modulus
N_c	Bearing capacity factor, cohesion
N_c^0	Bearing capacity factor, undrained conditions
N_q	Bearing capacity factor, overburden pressure
N_γ	Bearing capacity factor, unit weight
p_{active}	Active pore pressure
p_w	Pore water pressure
s_u	Undrained shear strength
$s_{u,inc}$	Linear increase of undrained shear strength with depth
w_{ef}	Effective foundation width
w_L	Liquid limit
q	Overburden pressure at foundation level
q_f	Bearing capacity

Greek letters

γ	Unit weight
γ'	Effective unit weight
$\Delta\gamma_s$	incremental deviatoric strain
ν	Poisson's ratio
ξ_c	Correction factor, cohesion
ξ_q	Correction factor, overburden pressure
ξ_γ	Correction factor, unit weight
σ'	Effective stress
σ_c	Preconsolidation pressure

σ_{v0}	Initial vertical overburden pressure
φ	Friction angle
ψ	Dilatancy angle

Abbreviations

CAUC	Consolidated Anisotropic Undrained Compression
CAUE	Consolidated Anisotropic Undrained Extension
DSS	Direct shear stress
MC	Mohr-Coulomb
OC	Overconsolidated
OCR	Overconsolidation ratio

1 Introduction

Cranes are used for piling and lifting and are therefore an essential part of the construction industry. Heavy machines coupled with poor ground conditions can however cause ground failures with machine damages and personal injuries as a consequence (Dahlgren & Edstam, 2017). Measures must therefore be taken to prevent cranes from overturning, gliding or causing other unintentional ground failures. Proper dimensioning of measures to prevent these type of accidents is not always done, and about two cranes overturns in Scandinavia every year.

When analyzing the bearing capacity of soft soil suffering from the weight of a heavy machine, good knowledge of soil properties and layering is essential (Dahlgren & Edstam, 2017). A number of aspects are important to analyze in order to create a safe system:

- The load from the machine
- The eventual load spreading system
- The eventual working platform
- The eventual dry crust
- The soft clay
- The geotechnical bearing capacity
- Handling of insecurities
- Communication at the construction site

This study will focus on the load from the machine, the working platform, the soft clay and the geotechnical bearing capacity.

1.1 Background

Dimensioning of crane foundations on soft soil is usually performed with analytical equations. According to IEG, the recommended method for calculating vertical bearing capacity is the general bearing capacity equation (IEG, 2010). The method was developed for hand calculations and may have simplifications that in some cases can be too conservative. Today, with user-friendly finite-element programs, such as PLAXIS, more complex problems can be studied numerically.

The background to this study is that the general bearing capacity equation is believed to be too conservative in the case of a working platform overlying soft soil.

1.2 Aim and objectives

The main objective of this study is to evaluate whether the general bearing capacity equation can be used to properly model crane foundations on working platforms of fill overlying soft clay. Furthermore, the intention is to give guidance for dimensioning of bearing capacity where the general bearing capacity equation is applicable or too conservative.

1.3 Methodology

The study started with a literature study concerning clay properties, working platforms, bearing capacity, crane foundations and the software PLAXIS. The literature study was followed by analytical calculations with the general bearing capacity equation for a hypothetical case. The bearing capacity of an isotropic soft clay profile was analyzed for varying fill thicknesses of the working platform.

Finite-element analyses were then performed for the same conditions as for the analytical calculations and the results were compared. After completing the study of a isotropic clay profile, finite-element analyses were performed for the case of a typical soil profile in the Gothenburg area. Here, the positive effects on bearing capacity caused by shear strength anisotropy of clay and the increase of shear strength with depth were studied. Finally, based on the results for the study, conclusions and recommendation for dimensioning of crane foundations on soft clay were given.

A detailed explanation of the analyses and chosen soil parameters can be found in section 6.

1.4 Scope

Analytical calculations are only performed with the general bearing capacity equation. Other analytical methods are not considered. The general bearing capacity equation is used in its original form in order to keep the soil model as simplified as possible. No correction factors need to be used. The crane load is modelled as a uniform vertical line load acting over the effective width of one or two crane tracks. No crane mats are used. The crane foundation is treated as a strip footing with plain strains conditions.

PLAXIS simulations are only conducted in two dimensions. All PLAXIS simulations are performed with a plain strain model instead of an axisymmetric model. The modelling of crane foundations on soft soil is considered a short-term stability problem during undrained conditions. Therefore, consolidation of the clay is not taken into account.

2 Soil properties

In this section the soil type included in the study is presented in regards to shear strength. Anisotropy, working platforms and drainage conditions will be explained in regards to bearing capacity.

2.1 Cohesive soils

Cohesive soils are defined as fine-grained soils consisting of a majority of clay minerals (Dahlgren & Nyman, Working Platform on Soft Clay, 2015). The term cohesion describes the strength of cohesive soils and is the force that binds clay particles together by molecular attraction forces. The cohesion is determined by the negative water pressure in the voids and the cementation between the particles.

The shear strength of cohesive soils can be divided into physical and chemical-physical forces (Dahlgren & Nyman, Working Platform on Soft Clay, 2015). The physical forces are a result of resistances from when particles slide against each other and the interlocking between particles. The chemical-physical forces are the cohesion and is as mentioned the attraction force between the particles. The shear strength of cohesive soils are usually rather low compared to friction soils.

Cohesive soils have low permeability, which means that the ground conditions are highly dependent on the existing drainage conditions (Dahlgren & Nyman, Working Platform on Soft Clay, 2015). The undrained shear strength of clay is a common parameter to obtain from different tests, and is influenced by the development of excess pore pressures. This indicates that cohesive soils are water sensitive.

For soft clay in areas where no loading has occurred other than the self-weight of the soil, it is common to find overconsolidated behavior (Olsson, 2013). In Sweden, an evaluation from an oedometer test according to the Swedish standard acquired an overconsolidation ratio (OCR) of 1.1-1.3. This means that the standard Swedish clay is considered slightly overconsolidated.

2.2 Dry crust

The upper part of a clay soil will be exposed to physical and chemical stresses (Grahnström & Jansson, 2016). As a result of this, a phenomena called surficial clay crust, or dry crust clay, will develop. The dry crust clay may show different properties than normal clay and is expected to be highly inhomogeneous in terms of shear strength and water content.

A sample testing of dry crust clay performed at Chalmers University of Technology in 1984 showed that the crust is characterized by higher shear strength and low water content than the underlying clay (Grahnström & Jansson, 2016). The dry crust is however sensitive to seasonal changes, with hydraulic properties decreasing as much as 75 percent during heavy rain.

In Gothenburg, the general depth of the dry crust is around zero to two meters deep, and show a significantly increase in shear strength compared to the underlying clay, with the unit weight being same (Larsson, o.a., 2007).

The impact of dry crust clay in soil stability have led to different approaches in geotechnical design (Grahnström & Jansson, 2016). Utilizing the full thickness of the dry crust clay and its geotechnical properties could lead to ground failures (Broms & Flodin, 1981). Instead, the dry crust could be divided into three parts with unique strength parameters to work around the high deviation in test results. Another approach is to use half of the dry crust thickness in bearing capacity calculations.

The current practice in calculating the bearing capacity of fill above clay is, as mentioned, the general bearing equation (IEG, 2010). This analytical solution does not account for dry crust clay. Hence, this study will not account for dry crust clay.

2.3 Working platforms of fill material

Before operating heavy vehicles such as pile driving crawler cranes, the soil area for the project has to be prepared in order to handle the load (Hercules, 2017). Correctly prepared soil will lead to a more efficient and safe construction site. Fill material can be applied on top of soils such as soft clay to stabilize the soil and to distribute loads in a favorable way.

The main difference between constructing a foundation on compacted fill material and natural soil is that the soil properties for fill material can be partly determined (IEG, 2010). Natural soil has certain unchangeable properties to account for when constructing a foundation while fill material can be selected to meet the desired specifications.

The planning and dimensioning of compacted working platforms includes consideration of geometric design, selection of fill material and placement method (IEG, 2010). According to IEG guidelines, fill material used for working platforms is usually referred to as natural soil, crushed rock or blasted rock. The fill material considered in this study will be blasted rock with empirically determined properties.

It is favorable to choose the foundation level so that a minimal amount of fill material is required (IEG, 2010). At the same time the fill layer should be thick enough to be uniform for the whole construction site. The minimal recommended thickness is therefore 0.3 meter. On the other hand, very thick fill layers will cause settlements due to the material weight. According to IEG, the thickness should not exceed 3-6 meter, highly depending on the given situation. Hercules presents a more specific recommendation based on soil type and shear strength, where the fill for soft clay ranges from 0.3 to 0.9 meter (Hercules, 2017).

To prevent finer material from penetrating coarser material it is necessary to put a material separating layer between the compacted fill and the underlying soil (IEG, 2010). For crane foundations on clay, a separating layer is needed between the fill material and the clay layer. If that is disregarded, settlements will likely occur due to movements in the interface between the soil and the fill. Drainage is another element that has to be considered, depending on if the fill material is water sensitive or not.

When fill material for a foundation on clay consists of crushed material or blasted rock, a material separating layer with a thickness of 0.2 m should be used (IEG, 2010). The layer could consist of crushed rock of various fractions, 0-65 mm.

Despite the recommendations in IEG, a material separating layer will not be included in the analysis of this study. Such a layer is not taken into account by the analytical equations in focus of the study and is therefore not included in PLAXIS either.

2.4 Drainage conditions

The shear strength of a soil is related to the drainage condition; an undrained soil does not have the same shear strength as a drained soil (Craig & Knappett, 2012). It is important to understand which drainage condition that a soil is experiencing in order to analyze the strength parameters in geotechnical practice correctly.

Clay is regarded as a fine-grained soil with low permeability (Craig & Knappett, 2012). The lower permeability a soil has, the longer time it takes for excess pore pressures to dissipate. This process is also known as consolidation. In a geotechnical analysis, the rate of stress change caused by loads from construction has to be put in relation to the rate of consolidation.

Loading on clay in the short-term (order of weeks or less) will be undrained while loading in the long-term will be drained (Craig & Knappett, 2012). From a construction point of view, for a low permeable soil, short-term refers to the construction time while long-term refers to the design life of a construction (order of tens of years).

Since this study covers the load of a crane, acting as a temporary structure during the construction phase, the clay underneath will be treated as an undrained material.

2.5 Anisotropy

Anisotropy is a term that can be defined as being directionally dependent (Yang & Du, 2016). It is the opposite of isotropy, which means uniformity in all directions. The similar term homogeneous means that the property is not a function of position. Isotropic is always homogeneous but the reverse is not true. Soil and rocks are widely regarded to show anisotropic and non-homogeneous behavior due to influence of external and internal environmental factors. However when calculating the bearing capacity of a foundation on soil, most theories are assuming isotropic and homogeneous media.

2.6 Undrained shear strength in soil

The undrained shear strength in soil depends on soil type, loading type, preconsolidation pressure and overconsolidation ratio (Larsson, o.a., 2007). The general equation to calculate this empirically is presented as:

$$c_u = a\sigma_c OCR^{-(1-b)} \text{ or } c_u = a\sigma_{v0} OCR^b \qquad \text{(Eq. 1 \& 2)}$$

Where *a* and *b* are parameters depending on the soil and load type.

The undrained shear strength is varying depending on the direction of the load (Larsson, o.a., 2007). In design the shear strength is divided into three zones: compression (active zone), direct and extension (passive zone), as seen in Figure 1:

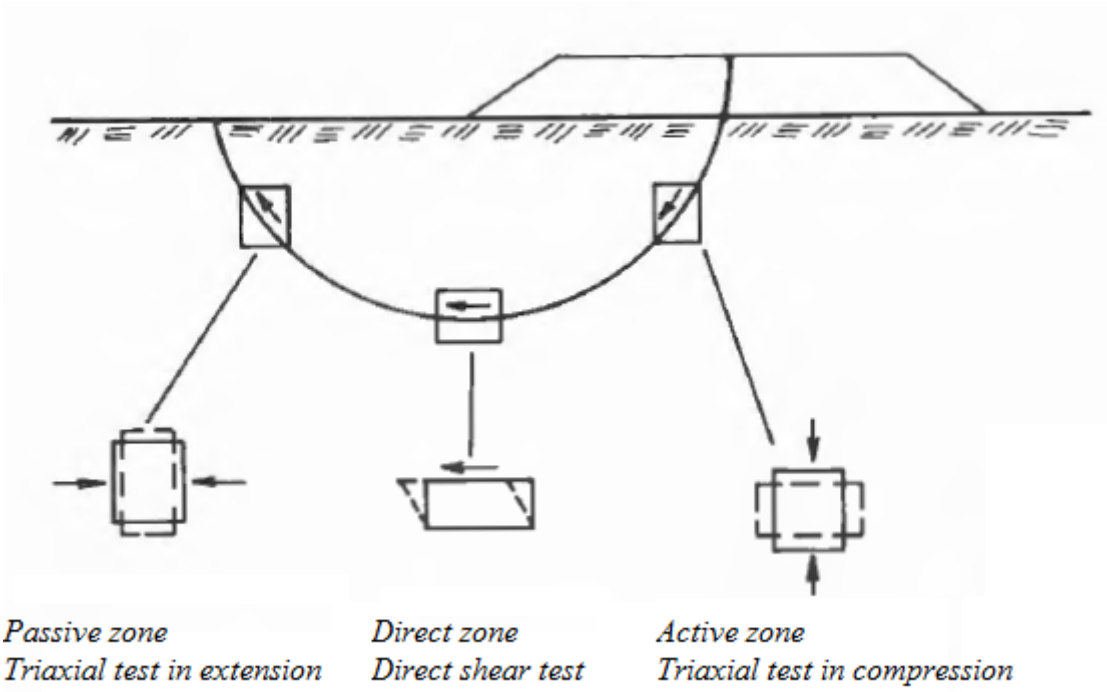

Figure 1: Active, direct and passive shear strength (Larsson, o.a., 2007)

To account for the different modes of shear strength in clay, the parameter of a is changed in the Swedish empirical solution as follows:

Active shear strength: $a{\sim}0.33$

Direct shear strength: $a{\sim}0{,}125 + 0{,}205\frac{w_L}{1.17}$

Passive shear strength: $a{\sim}0{,}055 + 0{,}275\frac{w_L}{1.17}$

The values above can be used for clayey silt as well, but for other soil materials, an empirical solution to account for the different shear strength is not obtainable (Larsson, o.a., 2007). The value of the parameter b is found to vary between 0.7-0.9 and is normally assumed to be 0.8.

The empirical relationship between the shear strength may vary and should never replace field tests, but instead work as a complement (Larsson, o.a., 2007). This study uses the relationship between shear strengths from field tests located in Utby, Gothenburg.

3 Bearing Capacity

Bearing capacity q_f is defined as the foundation pressure which would cause shear failure of the soil below or adjacent to a foundation (Craig & Knappett, 2012). The theoretical maximum pressure that can be applied without causing shear failure can also be referred to as ultimate bearing capacity. This definition indicates that the shear strength of a soil is strongly related to its bearing capacity. In geotechnical practice, bearing capacity can be regarded as the maximum load that can be applied on a foundation without causing soil collapse.

A conceptual model is required to evaluate the combined bearing capacity of a working platform with an underlying layer of clay (Dahlgren & Edstam, Som Man Bäddar Får Man Ligga, 2017). Given that the ground surface is horizontal, the failure mechanism is usually expected to be of local shear failure.

However, the situation is complicated since the soil supporting a foundation usually consists of a relatively thin and thick layer (a working platform or a dry crust) with soft clay underneath (Dahlgren & Edstam, Som Man Bäddar Får Man Ligga, 2017). The failure mechanism can either be completely contained in the thicker sublayer or in both the thick layer and the soft clay. It mainly depends on the relationship between the horizontal load spread, the thickness of the layers and their relative shear strength.

To date there is no generally adopted conceptual model in Sweden that accounts for this type of problem in a rational way (Dahlgren & Edstam, Som Man Bäddar Får Man Ligga, 2017). Instead, the effect of the working platform is often considered as a load spreading and the bearing capacity of the clay is calculated with the general bearing capacity equation.

3.1 Failure modes in soil

There are three different failure modes describing the shear failure of a soil; general shear failure, local shear failure and punching shear failure (Craig & Knappett, 2012). Which failure mode a soil will experience when the bearing capacity is exceeded depends on the material properties in terms of shear strength and stiffness.

General shear failure is a failure mode that is typical for low compressibility soils, such as dense coarse-grained and stiff fine-grained soils. The failure progresses from initial failure surfaces between the edges of the footing and the ground surface, to ultimately when the value q_f is reached, spreads downwards and outwards. Heaving occurs on both sides of the foundation which pushes the deformation to the sides. (Craig & Knappett, 2012). A general shear failure is illustrated in Figure 2.

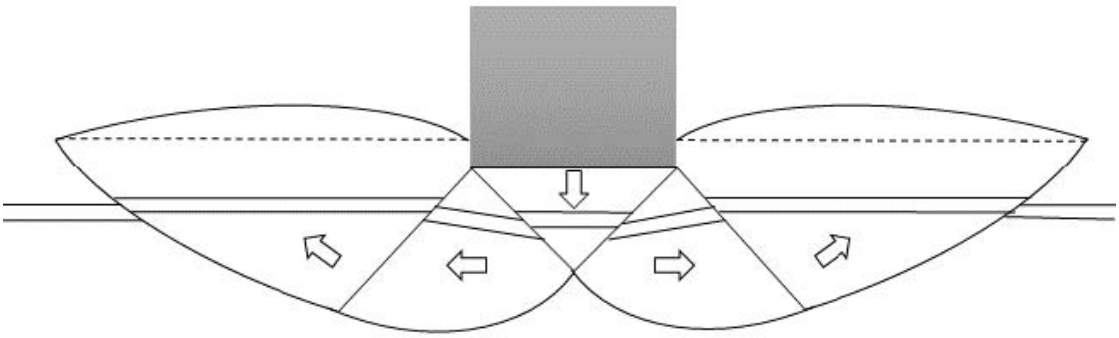

Figure 2: General shear failure (Grahnström & Jansson, 2016)

Local shear failure occurs in a soil which possess a high amount of compressibility. As a result of the soil compressing, the failure does not reach the ground surface as much as the previously mentioned case. The failure presents itself as relatively large settlements and slight heaving on the sides. (Craig & Knappett, 2012). A local shear failure is illustrated in Figure 3.

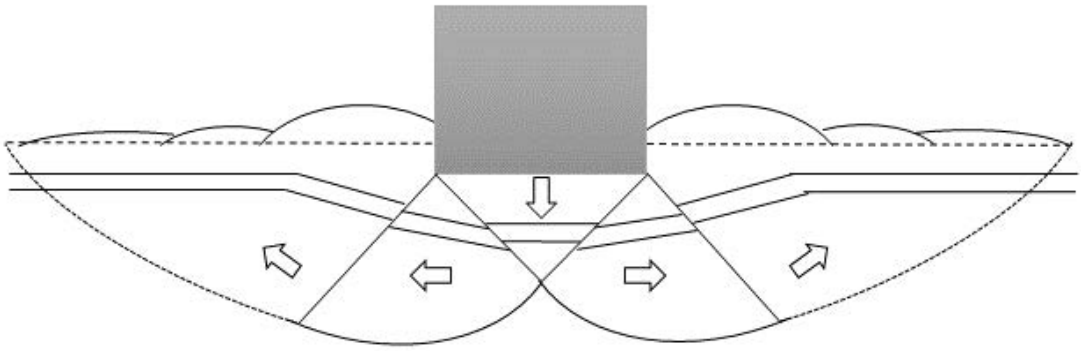

Figure 3: Local shear failure (Grahnström & Jansson, 2016)

Punching shear failure occurs in soils which possess a relatively high amount of compressibility, combined with shearing in the vertical direction around the edge of the footing. There is no heaving in this failure mode, and the settlements are relatively large and are located beneath the footing. (Craig & Knappett, 2012). A punching shear failure is illustrated in Figure 4.

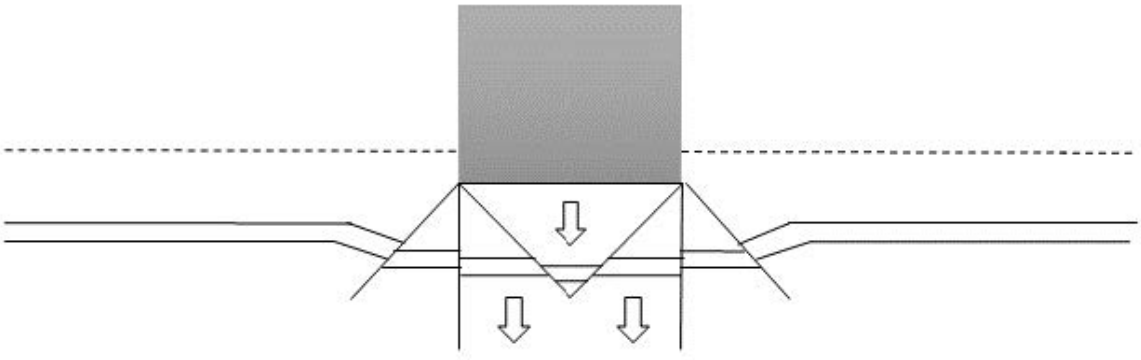

Figure 4: Punching shear failure (Grahnström & Jansson, 2016)

3.2 The General Bearing Capacity Equation

The general bearing capacity equation is based on Prandtl's original equation for calculating ultimate bearing capacity in 1921 (Murthy, 2003). Prandtl assumed a weightless material with friction and cohesion. Terzaghi developed the theory in 1943 to make it applicable for general shear failures of shallow strip footings. He took the overburden pressure into account by using an equivalent surcharge load at the base of the foundation.

Hansen added correction factors for the equation in 1961 to account for the load inclination, eccentricity, foundation depth and foundation shape (Bergdahl, Malmborg, & Elvin, Plattgrundläggning, 1993). Several other correction factors have been suggested over time, including factors by Hansen (1973), Vesic (1973) and Brown & Meyerhof (1969) to account for inclined ground surface, inclined foundation surface and the effect of looser soil within a certain distance from the foundation level.

There is no accurate analytical solution for the bearing capacity of footings, since the set of equations describing the yield problem of footings are nonlinear (Murthy, 2003). Instead, the correction factors are empirical factors based on experimental data and the many solutions suggested by different experts are very similar to Terzaghi's equation.

The general bearing capacity equation is presented below (Bergdahl, Malmborg, & Elvin, Plattgrundläggning, 1993):

$$q_f = cN_c\xi_c + qN_q\xi_q + 0.5\gamma' w_{ef} N_\gamma \xi_\gamma \qquad \text{(Eq. 3)}$$

Where $N_c^0 = \pi + 2 \; when \; \varphi = 0 \; (undrained \; conditions)$

$N_c = \left(N_q - 1\right)\cot(\varphi) \; when \; \varphi \neq 0$

$N_q = \frac{1+\sin(\varphi)}{1-\sin(\varphi)} e^{\pi * \tan(\varphi)}$

$N_\gamma = F(\varphi)\left[\frac{1+\sin(\varphi)}{1-\sin(\varphi)} e^{\left(\frac{3\pi}{2}\tan(\varphi)\right)} - 1\right], where \; F(\varphi) = 0.08705 + 0.3231\sin(2\varphi) - 0.04836 sin^2(2\varphi)$

In its original form, the general bearing capacity equation is only derived for a plane strain foundation at ground level with a centric vertical load (Bergdahl, Malmborg, & Elvin, Plattgrundläggning, 1993). Multiplying the bearing capacity factors (N_c, N_q, N_γ) with corrections factors (ξ_c, ξ_q, ξ_γ) will account for exceptions from that case.

The first term of the equation represents the contribution to the bearing capacity from the soil cohesion (Bergdahl, Malmborg, & Elvin, Plattgrundläggning, 1993).The second term is the contribution from the overburden pressure at the foundation level and the third term is the contribution from the unit weight of the soil wedge under the foundation during shear failure. An illustration of the three terms in relation to bearing capacity is presented in Figure 5:

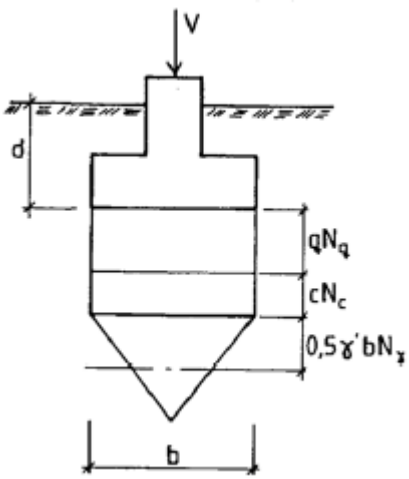

Figure 5: Bearing capacity – principle structure (Bergdahl et al. 1993)

3.2.1 Bearing capacity for cohesion soil

For cohesion soil, it is normal to assume $\varphi=0$ (Bergdahl, Malmborg, & Elvin, Plattgrundläggning, 1993). The assumption means that the third term of the general equation is neglected since $N_\gamma=0$. The material is regarded as "weightless" and the unit weight of the soil is not contributing to the bearing capacity. Additionally, $N_q=1$ and $N_c^0=\pi+2$. For a shallow foundation on undrained material, the general bearing capacity can be expressed as:

$$q_f = cN_c\xi_c + qN_q \qquad \text{(Eq. 4)}$$

3.2.2 Bearing capacity for friction soil on top of clay

When friction soil is overlying clay, such as fill material for crane foundations, the relationship between friction layer depth d and foundation width w_{ef} determines the method for calculating bearing capacity (Bergdahl, Malmborg, & Elvin, Plattgrundläggning, 1993). If the depth from the bottom of the foundation to the bottom of the friction layer is greater than 3.5 times the foundation width, the clay layer is not considered to affect the bearing capacity. The bearing capacity is then calculated for the friction soil only.

If h is less than 3.5 times w_{ef}, the bearing capacity is calculated according to Tcheng's equations from 1957 (Bergdahl, Malmborg, & Elvin, Plattgrundläggning, 1993). For the equation to be valid, it is assumed that a shear failure in the friction soil is not reducing the bearing capacity. Tcheng's equations are calculated as:

$$q_f = N_c^*\xi_c s_u \text{ when } 0 < \frac{d}{w_{ef}} < 1.5 \qquad \text{(Eq. 5)}$$

Where $N_c^* = 4\left(1 + \frac{d}{1.5*w_{ef}}\right)$

$$q_f = N_c^{**}\xi_c s_u + 0.5\gamma' b_{ef} N_\gamma^* \xi_\gamma \qquad \text{when } 1.5 < \frac{d}{w_{ef}} < 3.5 \qquad \text{(Eq. 6)}$$

Where $N_c^{**} = 4.5(3.5 - \frac{d}{w_{ef}})$

And $N_\gamma^* = 1.38\left[\sqrt{\frac{h}{b_{ef}}} - 1.23\right] N_q$

Where N_q is determined for friction soil; $N_q = \frac{1+\sin(\varphi)}{1-\sin(\varphi)} e^{\pi * \tan(\varphi)}$

For Eq. 5 only soil cohesion contributes to the bearing capacity, with a reworked N_c-factor which empirically incorporates the friction layer depth *d*. For Eq. 6, the contribution from the unit weight of the soil wedge during shear failure is also taken into account. The N_c and N_γ factors are both reworked. The contribution of overburden pressure is neglected in both cases.

The fact that only soil cohesion is considered to contribute to bearing capacity when the friction layer depth is less than 1.5 times the foundation depth might make the equation conservative. It is of interest to investigate if the reworked N_c-factor describes the bearing capacity accurately and if it is correct to neglect the unit weight of the friction soil.

The set of equations presented by Tcheng have nonlinear solutions. The values of bearing capacity are questionable around the ratio limit values 1.5 and 3.5. Comparing the different equations around limit values for certain soil and foundation properties could give different solutions. It is of interest to compare Tcheng's equations to finite element modelling to see if the nonlinearity remains or not.

3.3 Limit State Concepts

To analyze a structure's stability, the maximum load on the soil without causing failure is predicted (Sloan, 2013). This load is then divided by a safety factor, depending on the structure. Lower value of the safety factor is appropriate for slopes and higher values for foundations. When the ultimate load is determined, an analysis of the working deformations are done usually with some form of settlement evaluation.

When doing the stability analysis, you can generally choose between four different methods: limit equilibrium, limit analysis, finite-element programs and slip-line methods.

3.3.1 Limit equilibrium

Limit equilibrium is the oldest method used to evaluate stability (Sloan, 2013). It was first applied in 1773 by Coulomb. When used, the failure mechanism is predicted in advance, and calculations are made using the traditional strength parameters c and φ. The method has been widely used in history of geotechnics.

The disadvantage of the method is that the failure mechanism has to be guessed in advance, and if the prediction is incorrect it will result in poor estimations of the failure load.

The general bearing capacity equation is an adaption of the limit equilibrium methods created by Terghazi in its first form.

3.3.2 Limit analysis

Determination of the maximum load can be done using a method called limit theorems of plasticity, limit analysis, to calculate the lower and upper bound for the load (Sloan, 2013). The model assumes small deformations, a perfectly plastic material and an associated flow rule.

Lower bound theorem: The lower bound to the maximum load occurs if a state of stress can be found which does not exceed the failure criterion. Equilibrium with external load which includes soil weight should be present, thus no collapse can occur.

Upper bound theorem: If a mechanism of plastic collapse is kinematically admissible and the external load is equal to the power dissipated by the internal stresses, a collapse is occurring. The external load in this scenario constitutes an upper bound to the collapse load.

3.3.3 Finite-element analysis

Limit theorems can be applied to simple problems to give an analytical answer to the bounds, although the future strength lies in giving numerical formulations to more complex problems with finite-element programs (Sloan, 2013). New technologies and development of user-friendly software have resulted in finite-element programs being widely used in geotechnical practice.

There are two different approaches in finite-element analysis: displacement finite-element analysis and finite-element limit analysis.

Displacement finite-element analysis is used for predictions of deformations and stability, and can be applied for two different modes:

a. Increments of loads are applied to the soil until the program indicates a state of collapse due to the deformation response. The safety factor is obtained in terms of force.
b. Strength reduction analysis. The strength is reduced until equilibrium cannot be maintained. The soil is monitored with control points and gives a safety factor in terms of strength.

Properties for the mentioned limit states concepts in this section are presented in Table 1:

Table 1: Properties of the limit state concepts (Sloan, 2013)

Property	Limit equilibrium	Upper-bound limit analysis	Lower bound limit analysis	Displacement finite-element analysis
Assumed failure mechanism?	Yes	Yes	-	No
Equilibrium satisfied everywhere?	No (globally)	-	Yes	No (nodes only)
Flow rule satisfied everywhere?	No	Yes	-	No (integration points only)
Complex loading and boundary conditions possible?	No	Yes	Yes	Yes
Complex soil models possible?	No	No	No	Yes
Coupled analysis possible?	No	No	No	Yes
Error estimate?	No	Yes (with lower bound)	Yes (with upper bound)	No

4 Crane Foundations

Cranes are important tools in construction with the purpose of moving heavy materials with help of pulleys and cables. There are a number of different crane types used for various construction purposes. In this Thesis, the focus will be on crawler cranes since they are commonly used in construction sites consisting of soft soils (Dahlgren & Edstam, Som Man Bäddar Får Man Ligga, 2017).

Crawler cranes are movable with tracks attached at the bottom (Dahlgren & Edstam, Som Man Bäddar Får Man Ligga, 2017). The tracks provide enough stability on their own, hence outriggers are not required. The tracks also makes it possible for a crawler crane to move in sites with soft soils. The lifting capacity is very high with an average range of 40 to 3500 tons.

This study will focus on a specific crawler crane from the Finnish company Junttan. The model is called Junttan PM 23LC and is used as a piling machine. The specifications of the crane are presented in Table 2 (Junttan, 2017). An illustration of the crane geometries is presented in Figure 6.

Table 2: Weight of the crane (Junttan, 2017)

Machine without working equipment	47 100 kg
Counterweight	6000 kg
Drill head JD 1,5	600 kg
Rooter (HHK 3AS)	6000 kg
Total weight	**60 300 kg**
Rooter (HHK 4AS)	7800 kg
Total weight	**61 500 kg**
Rooter (HHK 5AS)	9100 kg
Total weight	**62 800 kg**

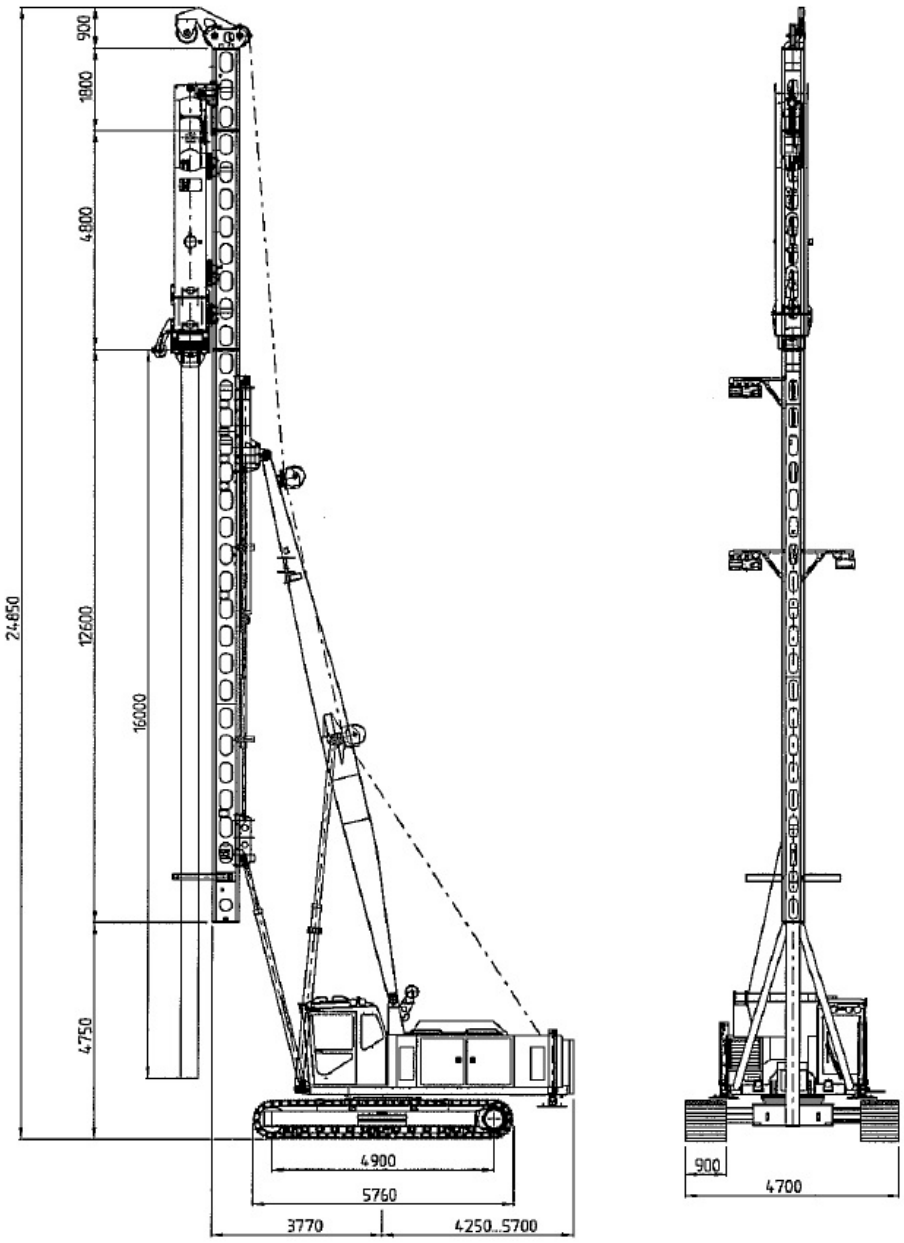

Figure 6: Junttan PM 23LC (Junttan, 2017)

4.1 Modelling the crane

When analyzing the bearing capacity of the soil, the tracks on the crawler crane are modelled as two uniform loads representing the two tracks. The dimensions are presented in Figure 6, 900 x 4900 mm. The value of the load is represented by the weight of the crane.

In PLAXIS 2D, the tracks are modelled with the shortest length, in this case 0.9 m, to get the most critical case.

4.2 Load Conditions

When analyzing the load caused by a piling crane, there are different load conditions based on what direction the piling system is pointed (Dahlgren & Edstam, Som Man Bäddar Får Man Ligga, 2017). Additionally, when a piling crane is in action, the crane system is moving, causing different loading cases. The center of gravity is located at a high elevation in relation to the ground, which leads to a rickety system.

The load conditions could be divided into three different ones, as seen in Figure 7 (Dahlgren & Edstam, Som Man Bäddar Får Man Ligga, 2017) .To the left, the carriage is located parallel to the tracks. In the middle, the carriage is located perpendicular to the tracks. To the right, the carriage is located diagonally to the tracks. The most critical case is where the carriage is located diagonally relative to the tracks. In thesis however, only the case where the carriage is located perpendicular to the tracks will be considered and the load will only be acting vertically over the tracks.

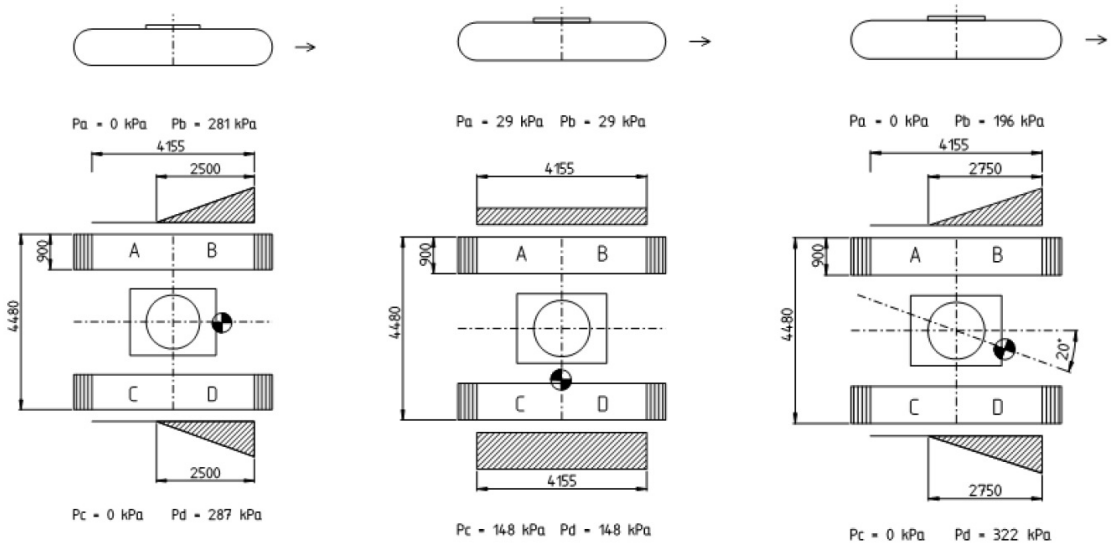

Figure 7: Three load conditions for a piling crane (Dahlgren & Edstam, Som Man Bäddar Får Man Ligga, 2017)

5 Software outline – PLAXIS 2D

Plaxis is intended for analysis of deformation and stability in geotechnical engineering and rock mechanics. The different application range from excavation, embankment and foundations to tunneling, mining and reservoir geomechanics. PLAXIS is available in 2D and 3D but only the 2D version is covered in this thesis.

5.1 Model selection

There are two options available for modelling finite-elements in PLAXIS 2D; *Plane strain* or *Axisymmetric* (Plaxis, 2017). Both options result in a two dimensional model with two degrees of freedom per node (x- and y-direction).

5.1.1 Plane Strain

A *Plane strain* model can be used for geometries with one relatively long dimension and a uniform cross section perpendicular to the long dimension (Karstunen, Geotechnical modelling III, 2016). The cross section has a similar stress state and loading at any length in the z-direction (out-of-plane direction). A consequence of the plane strain model is that displacements and strains in the z-direction are zero while normal stresses in the z-direction are considered (Plaxis, 2017). The plane strain model is illustrated in Figures 8 and 9:

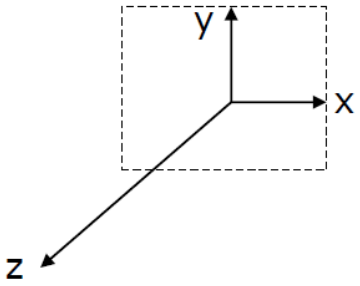

Figure 8. Plane strain model (Karstunen, Geotechnical modelling III, 2016)

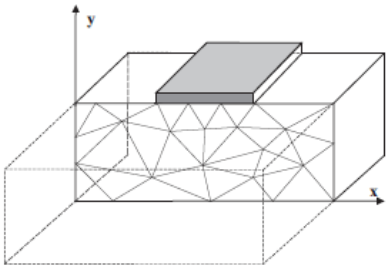

Figure 9: Plane strain model (Plaxis, 2017)

5.1.2 Axisymmetric

An *Axisymmetric* model can be used for circular geometries with a uniform radial cross section around the central axis (Karstunen, Geotechnical modelling III, 2016). The stress state and loading is the same in any radial direction. Stress and strain perpendicular to the central axis is radial. The y-axis in an axisymmetric model represents the axial line of symmetry while the x-coordinate represents the radius (Plaxis, 2017). The axisymmetric model is illustrated in Figures 10 and 11:

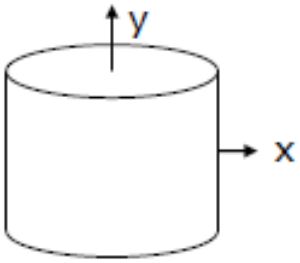

Figure 10: Axisymmetric model (Karstunen, Geotechnical modelling III, 2016)

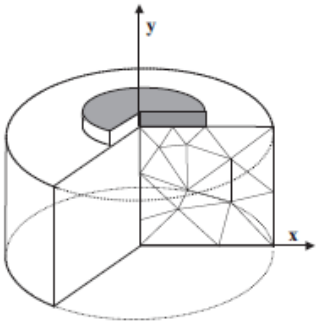

Figure 11: Axisymmetric model (Plaxis, 2017)

5.1.3 Selection for this Thesis

In this thesis a plane strain model was used with 15-node triangular elements, in favour of the less advanced 6-node system (Plaxis, 2017). The analytical solution for bearing capacity refers to a plane strain model and there were several reasons to use the same approach in PLAXIS.

Even though there are analytical shape factors to account for rectangular geometries where one dimension is not elongated, the comparison of the analytical equation and finite-element modelling can be performed by using the default plane strain options for both methods. The short dimension is the most critical one for bearing capacity.

Since the crawler crane has rectangular tracks, an axisymmetric model assuming a uniform radial cross section was not considered to be reasonable.

5.2 Material Model selection

The Mohr-Coulomb model is suitable for a first order approximation of stability problems and was used for the hypothetical study. NGI-ADP is considered the most appropriate standard material model in Plaxis for this study since it is applicable for a foundation with undrained loading on slightly overconsolidated clay. Importantly, it also incorporates the anisotropic behavior of clay in a simple manner. A NGI-ADP model was therefore used for the realistic case.

5.2.1 Mohr-Coulomb

The Mohr-Coulomb model is a simple linear elastic plastic model which serves as a good tool for a first estimate of the bearing capacity (Plaxis, 2017). It is based on the linear elastic theory from Hooke's law, and Mohr Coulomb's failure criterion. In order to find out if plasticity occurs, the function f, for yielding, is introduced and is dependent on the stress and strain. In the case of plastic yielding, $f = 0$.

The fundamental parameters of the Mohr-Coulomb model are presented in Table 3:

Table 3: Mohr-Coulomb parameters (Plaxis, 2017)

Parameter	Description	Unit
E'	Young's modulus	$\frac{kN}{m^2}$
ν'	Poisson's ratio	-
c'	Cohesion intercept	$\frac{kN}{m^2}$
φ'	Friction angle	°
ψ	Dilatancy angle	°

Young's modulus can be substituted with a shear modulus G or an oedometer modulus E_{oed} (Plaxis, 2017). It can also be substituted with a bulk modulus K (Dijkstra, Soil behaviour in shear , 2016). An elastic material can be completely described if two of the following parameter are known: *E'*, *G'*, *v'* or *K'*. Depending on the drainage type, the parameters are presented with a different symbol. Effective parameters are indicated by a prime sign (') and undrained parameters with a subscript u.

5.2.2 NGI-ADP

The NGI-ADP model is best suited to analyze conditions of undrained loading of clay (Plaxis, 2017). Capacity, deformation and soil-structure interaction can be evaluated from the results. The model is built on the basis as follows:

- Data of undrained shear strength of clay in three different stress states: active, direct simple shear and passive.
- A yield criterion which is based on an approximation of Tresca's criterion.
- Interpolation functions from an elliptical plot is done for plastic failure strains and for shear strengths in random stress paths.
- Isotropic elasticity, defined by the parameter G_{ur} (unloading/reloading shear modulus)

Parameters of the NGI-ADP model are presented in Table 4:

Table 4: Parameters of the NGI-ADP model (Plaxis, 2017)

Parameter	Description	Unit
G_{ur}/s_u^A	Ratio unloading/reloading shear modulus over (plane strain) active shear strength	-
γ_f^C	Shear strain at failure in triaxial compression	%
γ_f^E	Shear strain at failure in triaxial extension	%
γ_f^{DSS}	Shear strain at failure in direct simple shear	%
$s_u^A{}_{ref}$	Reference (plane strain) active shear strength	$\frac{kN}{\frac{m^2}{m}}$
$s_u^{C,TX}/s_u^A$	Ratio triaxial compressive shear strength over (plane strain) active shear strength	-
yref	Reference depth	m
$s_u^A{}_{inc}$	Increase of shear strength with depth	$\frac{kN}{\frac{m^2}{m}}$
s_u^P/s_u^A	Ratio of (plane strain) passive shear strength over (plane strain) active shear strength	-
τ_0/s_u^A	Initial mobilization	-
s_u^{DSS}/s_u^A	Ratio of direct simple shear strength over (plane strain) active shear strength	-
v'	Poisson's ratio	-

5.3 Undrained effective stress analysis

The undrained stress in PLAXIS can be analyzed using one of three different modes: *Undrained (A)*, *Undrained (B)* or *Undrained (C)*. Which mode to use depends on available parameter data and the material behavior of the soil layer (Plaxis, 2017). *Undrained (A)* and *Undrained (B)* are used to analyze effective stress while *Undrained (C)* is used to analyze total stress. Since *Undrained (C)* refers to a drained material behavior, it is not of interest for this study.

Pore pressures are contributing to the effective stress in a soil structure as stated in Terghazi's principle, with total stress resulting in effective stresses σ', active pore pressures p_{active} and pore water pressure p_w (Plaxis, 2017). However when analyzing the shear strength of a geostructure, the water is supposed to not sustain any shear stresses, hence the total shear stresses equals to the effective shear stresses.

5.3.1 Undrained A

In the case of *Undrained (A)*, effective strength parameters φ' and c' are used to model the material's undrained shear strength (Plaxis, 2017). The development of pore pressures are of importance in this mode to provide the accurate effective stress path that leads to failure at a realistic value of undrained shear strength (c_u or s_u).

A limitation to the use of PLAXIS is that most soil models are not capable of providing the correct effective stress paths in undrained conditions (Plaxis, 2017). Thus, defining the materials strength in effective strength parameters will often provide an incorrect value of the undrained shear strength.

5.3.2 Undrained B

If the undrained shear strength profile is known, an analysis of the undrained effective stress can be done by setting the friction angle to zero and the cohesion equal to the undrained shear strength ($\varphi=\varphi_u=0°$; $c=s_u$) (Plaxis, 2017). This is what defines *Undrained (B)*. Although the effective stress path and pore pressures may not be fully correct, the undrained shear strength will not be affected since it is specified as an input parameter.

Young's modulus will be an effective parameter in the cases of *Undrained (A)* and *Undrained (B)* with the incompressibility being taken care of automatically by PLAXIS (Plaxis, 2017). By setting $\varphi=\varphi_u=0°$ and $c=s_u$, the dilatancy angle ψ will also be zero. Furthermore, a friction angle of zero will lead to a change in failure criterion, from Mohr Coulomb to Tresca.

5.3.3 Selection for this Thesis

The drainage mode used in this Thesis was *Undrained (B)*. Since the undrained shear strength is an input parameter, it is a useful option for modelling stability problems in undrained conditions (Karstunen, Drained and Undrained Behaviour, 2016).

Having undrained shear strength as an input parameter is also a great advantage when comparing PLAXIS to the analytical equations, where undrained shear strength is an input parameter as well.

There is a large distinction between *Undrained (A)* and *Undrained (B)* where the first generates realistic pore pressures if the model is calibrated correctly while the latter does not (Karstunen, Drained and Undrained Behaviour, 2016). In other words, the first one is more suitable for consolidation and long-term analysis and the latter for short-term analysis. Additionally, *Undrained (A)* overestimates the undrained shear strength of clays which would have been very inappropriate for this study.

5.4 Bearing capacity in PLAXIS

Bearing capacity in PLAXIS was determined by increasing the line load representing the crane until the soil collapsed through a local, general or punching shear failure. The maximum load that could be handled by the soil without collapsing was set to the ultimate bearing capacity for a certain model. During the initial simulations of each model, a safety analysis was following the plastic phase in order to find the maximum load efficiently. A safety analysis in PLAXIS results in a factor of safety obtained by phi-c reduction (Plaxis, 2017).

6 Analysis

The first part of the analysis consists of a hypothetical case where analytical calculations and PLAXIS simulations were compared for a homogenous clay in terms of bearing capacity for varying thicknesses of fill. It was therefore of great importance that the conditions in PLAXIS resembled those of the analytical calculations. For this comparison, the clay was modelled with Mohr-Coulomb and the fill with Hardening Soil Small.

The second part consisted of a NGI-ADP model corresponding to a more realistic case of a Gothenburg Soil. Unlike the previous model, three major differences were implemented that are not covered in the analytical formula; soil anisotropy, linearly increasing undrained shear strength with depth and two effective widths due to two crane tracks. Instead of calculating the maximum bearing capacity, the load in the second part was corresponding to the crane model Junttan PM 23LC. The three implemented factors were investigated with the required fill thickness as a result. The fill was modelled with Hardening Soil Small, just like in the previous case.

The soil parameters used for the analytical calculations and the comparative simulations in PLAXIS were determined empirically to represent a soft clay in Gothenburg. For the NGI-ADP simulations where a realistic case is modelled, some soil parameters are derived from soil tests performed in Utby, Gothenburg. Unit weight and undrained shear strength of clay is consistent for all models during the analysis, deriving from typical Gothenburg values. The analyses are described in Table 5.

Table 5: Description of the analyses

Analysis	Approach	Focus of the analysis
Hypothetical case		
Analytical analysis	General Bearing Capacity Equation	Calculate q_f
PLAXIS analysis	Mohr-Coulomb clay HS small fill	Calculate q_f with conditions resembling the analytical analysis
Realistic case		
PLAXIS Analysis	NGI-ADP clay HS small fill Junttan PM 23LC crane	Calculate required fill 4 scenarios incorporating: -2 tracks -Anisotropy -$s_{u,inc}$

6.1 Hypothetical case

In this section, the hypothetical case with a comparison between analytical calculations and PLAXIS simulations for a isotropic clay is presented.

6.1.1 Analytical analysis

The analytical calculations were performed with Tcheng's equations from 1957 for an effective width w_{ef} of 0.9 m (Bergdahl et al. 1993) Eq. 4 was used in the case of no fill. Eq. 5 was used for fill thicknesses up to 1.35 m and Eq. 6 was used for fill thicknesses greater than 1.35 m and up to 3.15 m. The parameters used for the clay and the fill are presented in table 6 and 7.

Table 6: Clay parameters

Parameter	Description	Unit	Value	Acquired from
$\mathbf{S_u}$	Undrained shear strength	$\frac{kN}{m^2}$	10	Reasonable value for Swedish clay
$\mathbf{N_c}$	Bearing capacity factor	-	π+2	Plattgrundläggning
ξ_c	Correction factor	-	1	Assumed

Table 7: Fill parameters

Parameter	Description	Unit	Value	Acquired from
c	Cohesion	$\frac{kN}{m^2}$	0	Assumed
φ	Friction angle	°	45	TK Geo 13
ξ_γ	Correction factor	-	1	Assumed

6.1.2 PLAXIS analysis (Mohr-Coulomb)

In order for a PLAXIS model to be comparable to the analytical calculations it is necessary to consider a uniform clay layer with undrained shear strength constant with depth. Only one of the crane tracks can be modelled since only one effective width is taken into account in the formula. Shape factors are ignored and hence the crane is interpreted as a plain strain structure for both calculation methods.

The crane load was modelled as a line load acting over the effective width 0.9 m of one crane track. The maximum load that could be applied without causing failure was the result of interest for the comparison.

It was not obvious how to model the interface between the crane foundation and the soil in a correct way. The line load can be applied directly to the soil or with an underlying structure such as a plate. Since crane tracks can be regarded as relatively rigid structures, three cases were investigated initially; one case without any structural interface, one case with a plastic plate and one case with a rigid plate. Depending on the magnitude of the difference in bearing capacity outcome, one or more cases of interfaces may prove necessary to investigate further. The groundwater table is kept at 0 level, at the interface between the clay and the fill. The PLAXIS model is presented in Figure 12. The mesh of the model is presented in Figure 13.

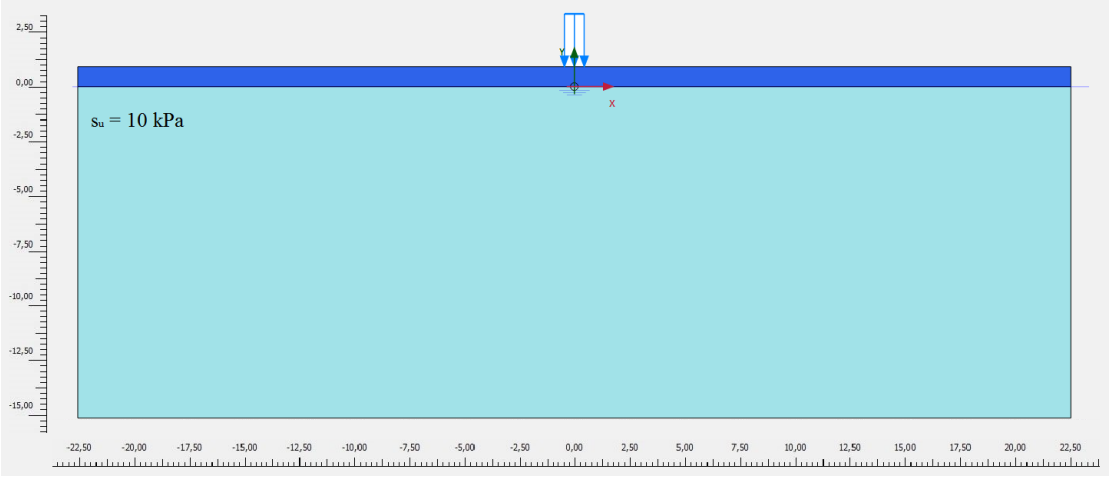

Figure 12: PLAXIS model with MC clay and HS small fill

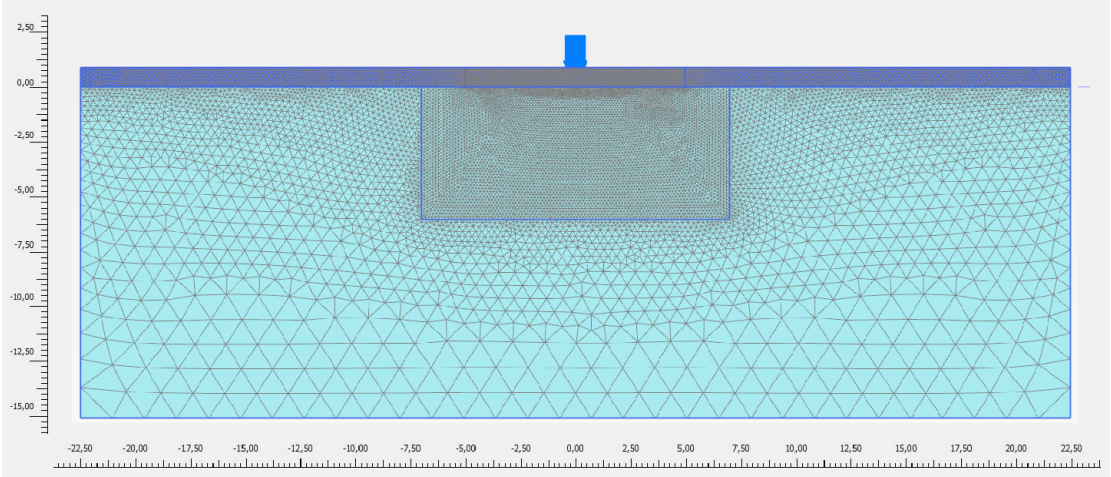

Figure 13: Mesh of the PLAXIS model

The material parameters used for clay, fill and plate are presented in Table 8, 9 and 10:

Table 8: Clay parameters (Mohr Coulomb)

Parameter	Description	Unit	Value	Acquired from
γ_d	Dry unit weight	$\frac{kN}{m^3}$	17	Reasonable value for Swedish clay
γ_s	Saturated unit weight	$\frac{kN}{m^3}$	17	Reasonable value for Swedish clay
E	Young's modulus	$\frac{kN}{m^2}$	$250c_u$	TK Geo 13
ν'	Effective Poisson's ratio	-	0.33	Reasonable value for Swedish clay
$s_{u,ref}$	Undrained shear strength	$\frac{kN}{m^2}$	10	Reasonable value for Swedish clay
φ	Friction angle	°	0	0 for *Undrained B*
ψ	Dilatancy angle	°	0	0 for *Undrained B*

Table 9: Fill parameters (Hardening Soil Small)

Parameter	Description	Unit	Value	Acquired from
γ_d	Dry unit weight	$\frac{kN}{m^3}$	19	TK Geo 13
γ_s	Saturated unit weight	$\frac{kN}{m^3}$	22	TK Geo 13
E_{50}^{ref}	Secant stiffness in standard drained triaxial test	$\frac{kN}{m^2}$	222.3	ELU
E_{oed}^{ref}	Tangent stiffness for primary oedometer loading	$\frac{kN}{m^2}$	222.3	ELU
E_{ur}^{ref}	Unloading/reloading stiffness from drained triaxial test	$\frac{kN}{m^2}$	1238	ELU
Power (m)	Power for stress-level dependency of stiffness	-	0.5	ELU
c'	Effective cohesion	$\frac{kN}{m^2}$	0.5	ELU
φ	Friction angle	°	45	TK Geo 13
ψ	Dilatancy angle	°	15	ELU
$\gamma_{0.7}$	Treshold shear strain at which $G_s=0.722G_0$	-	0.03E-3	ELU
G_0^{ref}	Reference shear modulus at very small strains	$\frac{kN}{m^2}$	525.6	ELU
ν'_{ur}	Effective Poisson's ratio for unloading-reloading	-	0.2	ELU

Table 10: Plate parameters

Parameter	Description	Unit	Value plastic plate	Value rigid plate	Acquired from
EA_1	Normal stiffness	$\frac{kN}{m}$	0.1	200	Assumed
EA_2	Stiffness in the out of plane direction	$\frac{kN}{m}$	0.1	200	Assumed
EI	Bending stiffness	$\frac{kNm^2}{m}$	0.1	200	Assumed

6.2 Realistic case PLAXIS analysis (NGI-ADP)

The NGI-ADP modelling was divided into four different scenarios which were calculated both for one and two crane tracks. The idea was to investigate the isolated and combined effects of two crane tracks, increasing shear strength with depth and anisotropic shear strength. As described in the crane specifications, each track has an effective width w_{ef} of 0.9 meter and the spacing between two tracks is 2.8 meter. The four scenarios are presented in Table 11. The anisotropic shear strength behavior and the shear strength increase with depth is presented in Figure 14. The NGI-ADP model with 2 tracks is presented in Figure 15. The model has the same mesh as for the Mohr-Coulomb model.

Table 11: Scenarios for the NGI-ADP model

Scenario	$S_u{}^A{}_{inc}$	Anisotropy
1	0	No
2	1.5	Yes
3	1.5	No
4	0	Yes

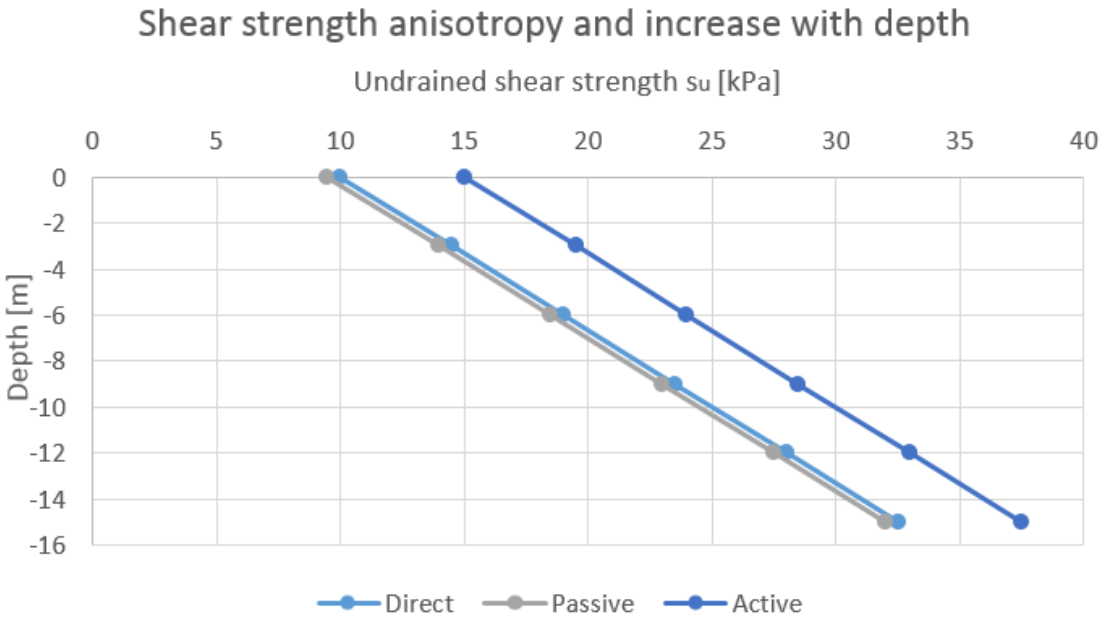

Figure 14: Shear strength anisotropy and increase with depth

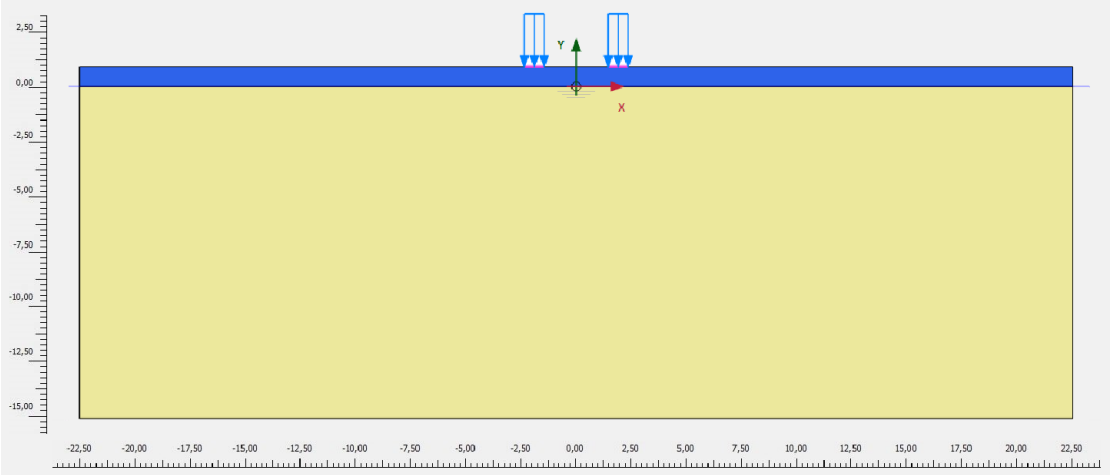

Figure 15: PLAXIS model with NGI-ADP clay and HS small fill

Stiffness parameters were derived from the paper *Consequences of sample disturbance when predicting long-term settlements in soft clay* (Karlsson, Emdal, & Dijkstra, 2017). The authors have been conducting laboratory tests of samples collected from a soft clay test site in Utby, Gothenburg. Results are presented from two different sampling methods; the Swedish piston sampler STII and a Norwegian mini-block sampler.

According to SGI, undisturbed sampling in Swedish cohesive soils is mainly carried out with the standardized piston samplers STI and STII (Bergdahl, Geotekniska undersökningar i fält , 1984). Both of the piston samplers have a sample diameter of 50 mm, sample length of 700 mm and a common edge angle. In this study, the soil data obtained from Utby with a STII sampler was used.

The unloading/reloading shear modulus G_{ur} was obtained from an undrained triaxial test in compression (CAUC) (Karlsson, Emdal, & Dijkstra, 2017). The ratio between passive and active undrained shear strength was gathered from undrained triaxial tests in extension (CAUE) and compression. The ratio of direct simple shear strength over active shear strength was assumed after careful consideration of empirical values, recommendations in the PLAXIS manual and discussion with experts.

The fill parameters are the same as in the previous case. The clay parameters used for clay are presented in Table 12. A more detailed description of how clay data was derived from the soil tests is presented in Appendix A.

Table 12: Clay parameters (NGI-ADP)

Parameter	Description	Unit	Value	Acquired from
γ_d	Dry unit weight	$\frac{kN}{m^3}$	17	Reasonable value for Swedish clay
γ_s	Saturated unit weight	$\frac{kN}{m^3}$	17	Reasonable value for Swedish clay
G_{ur}/s_u^A	Ratio unloading/reloading shear modulus over (plane strain) active shear strength	-	99.56	Soil tests from Utby
γ_f^C	Shear strain at failure in triaxial compression	%	1.33	Soil tests from Utby
γ_f^E	Shear strain at failure in triaxial extension	%	3.68	Soil tests from Utby
γ_f^{DSS}	Shear strain at failure in direct simple shear	%	2.05	Intermediate value
$s_u^A{}_{ref}$	Reference (plane strain) active shear strength	$\frac{\frac{kN}{m^2}}{m}$	15 (10)	Reasonable value for Swedish clay
y_{ref}	Reference deptg	m	0	Assumed
$s_u^A{}_{inc}$	Increase of shear strength with depth	$\frac{\frac{kN}{m^2}}{m}$	1.5 (0)	Reasonable value for Swedish clay
s_u^P/s_u^A	Ratio of (plane strain) passive shear strength over (plane strain) active shear strength	-	0.6333 (1)	Soil tests from Utby
s_u^{DSS}/s_u^A	Ratio of direct simple shear strength over (plane strain) active shear strength	-	0.6667 (1)	Assumed
ν'	Effective Poisson's ratio	-	0.33	Reasonable value for Swedish clay

6.3 PLAXIS work process and uncertainties

A vast amount of time doing this study was spent modelling in PLAXIS. The work process and uncertainties with the modelling in PLAXIS is listed below.

6.3.1 Clay layer with constant s_u of 10 kPa

The main concern during our work process in PLAXIS was to transfer the simplified conditions in the analytical solution to a simulation in PLAXIS. The bearing capacity analysis for a soft clay layer with s_u constant with depth turned out to be problematic for large fill thicknesses.

Initially the clay was modelled with a constant s_u of 10 kPa, with the fill on top. Unfortunately, the bottom of the clay layer experienced shearing and plastic points over the entire width as significant quantities of fill were applied. These failure points were present already in the Initial Phase in PLAXIS, before the crane load was applied. It seemed like the low undrained shear strength of the clay was unable to support the large weight of the fill material. The obtained failure points are presented in Figure 16.

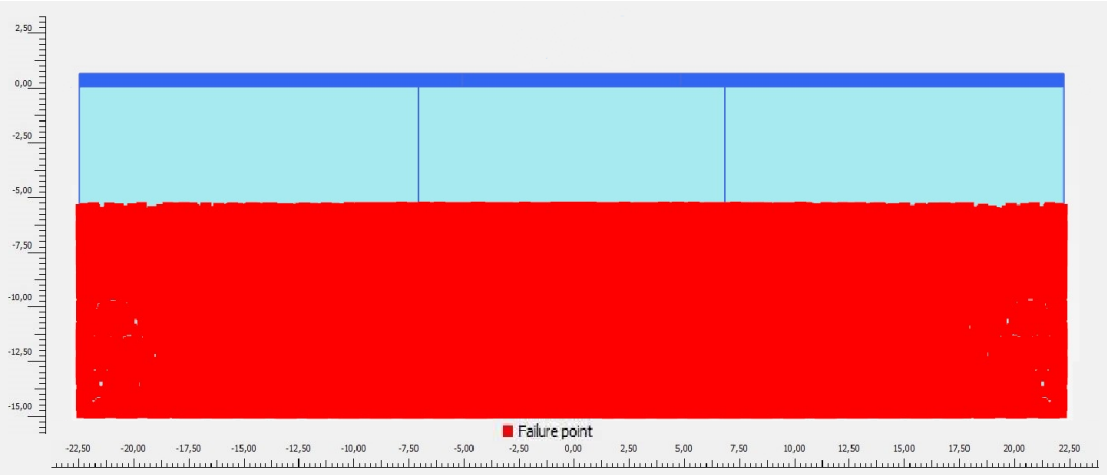

Figure 16: Failure points in the bottom of the clay

Even though PLAXIS highlighted this with a warning, the plastic calculation phase still proceeded and finished as normal. The bottom plastic points did not cause soil collapse and appeared to be unrelated to bearing capacity and the plastic points in the top of the clay layer caused by the crane load. It rather seemed like a symmetric settlement.

The problem was tackled by replacing the clay from -6 meter and downwards with a stronger clay layer with s_u 15 kPa and $s_{u,inc}$ 1.5 kPa/m, as in Figure 17. The stronger clay was not predicted to affect the analytic analysis and bearing capacity result since the failure caused by the crane load appeared in the top few meters of the clay.

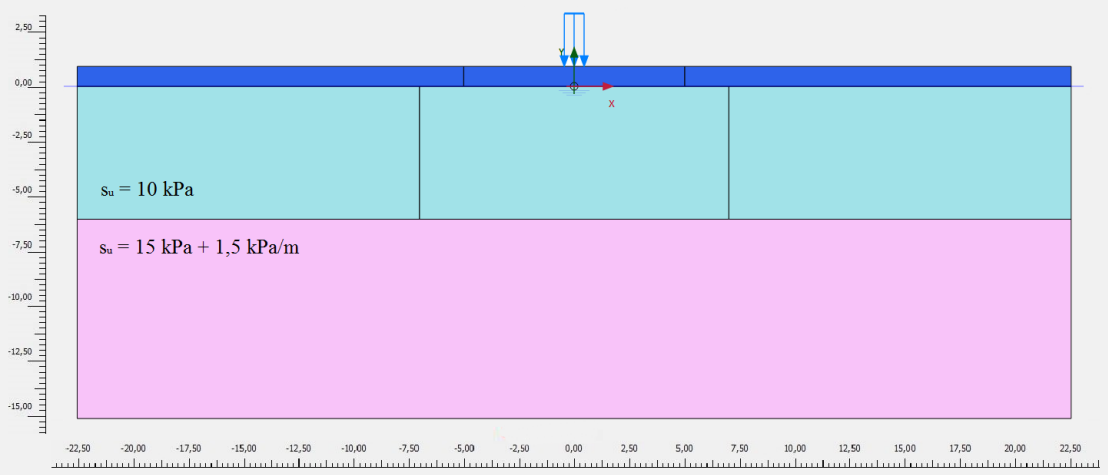

Figure 17: PLAXIS model with a stabilizing layer of stronger clay

However, as the thickness of the fill layer was increased, failure points in the bottom of the weaker clay layer appeared again, expanding upwards. It was inevitable that the failure points for thicker fill would reach the top of the clay layer and interfere with the failure points caused by the crane load. This started to occur for fill layers of 1.7 meter or thicker. At this point the fill thickness seemed out of proportion for the relatively weak clay with s_u 10 kPa, even with a stabilizing layer. The analysis of bearing capacity was therefore not proceeded for thicker fills.

The plastic points received at a fill thickness of 1.7 meter can be observed in Figure 18:

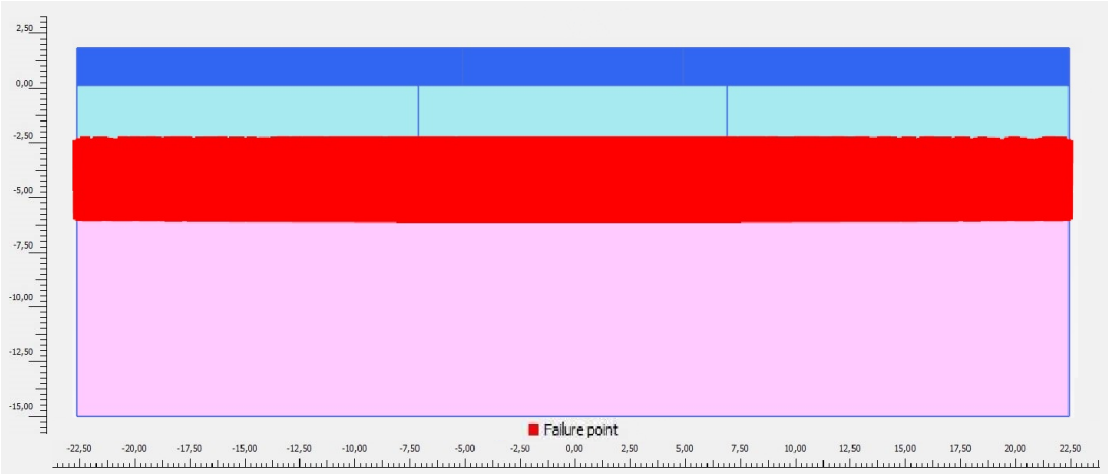

Figure 18: Plastic points close to the surface of the clay layer

6.3.2 Mohr-Coulomb modelled fill

After correcting the stability of the clay, the expectation was to receive reasonable values for bearing capacity; values close to the analytical solution. However, the bearing capacity of the geostructure was very low compared to the analytical solution. After studying the output results in PLAXIS, failure mechanisms were found in the fill.

A separate model consisting of only fill material down to -15 meter was made to analyze the bearing of it, and to evaluate if the previous results was reasonable. The results of this model indicated that the fill should be able to handle more load than the first results showed.

6.3.3 Change to HS Small modelled the fill

After studying the model recommendations in PLAXIS and getting input from experts in the field, the fill material was instead modelled with HS Small. HS Small required more input data and was considered to be a superior model in general. This proved to be a good move and lead to reasonable results. That was most likely due to more advanced stiffness parameters.

6.3.4 NGI-ADP stiffness

As stated in the analysis section, the NGI-ADP model is based on soil data from a test site in Utby. Shear strength and stiffness parameters were derived from a reference level of -6 meters. However, the decline in soil stiffness from the reference level to the surface could not be accounted for by the NGI-ADP model. Hence, some sort of simplification was required before being able to use the soil data. After discussing this matter with experts in the field, it was decided that the stiffness data for -6 meter could be used for a reference level of 0 meter. The value was still realistic and soil stiffness was not considered as important for the analysis as soil shear strength.

Another limitation with the NGI-ADP model is that it does not account for soil softening. Even though the deviatoric stress decreases significantly after failure is reached in a clay, the peak values for strength and stiffness are still used. This means that the model is unconservative in terms of undrained shear strength and stiffness for large strains. The plastic points obtained in the plastic calculations may therefore show an overestimated undrained shear strength and stiffness.

6.3.5 Numerical settings

When modelling relatively high fill thicknesses, the model consumed more time to find the accurate maximum load. A reoccurring issue when modelling was early failure with the error code: *Load advancement procedure fails*. This error code is explained shortly in Plaxis as a numerical problem, and you are recommended to inspect the input data and the calculation results in Output and try to find out why the model fails.

After being in contact with Plaxis, the recommendation was to tweak the following numerical settings:

1. *Increase the number of max. unloading steps*

This value gives the number of unloading steps that is allowed before the soil body is declared to have collapsed. This value can be altered in the case of a change in mechanism during the load time. The default value of this parameter is 5. When tweaking the model, the value was changed to 10.

2. *Increase the number of max. iterations*

This parameter only affects the calculation time of the model. If the maximum allowable number of iterations is reached in the final step of the calculation, an error code stating this will appear, hence this value was not changed.

3. *Limit the max load fraction step*

The calculation may perform too large load steps at a time and hence it needs to do large corrections when suddenly a lot of plasticity occurs in the model. This can result in load advancement procedure failure. The default value of this parameter is 0.8. When tweaking the model, this value was changed to 0.02.

Calibrating the models was the most time consuming part of this Thesis. Large variations in the bearing capacity results were obtained after changing the numerical settings. Therefore, it was important to determine reasonable setting that remained the same for all models included in the study.

6.3.6 Modelling time

With a calculation time of a PLAXIS model ranging between 15-60 minutes, correct calibration of the models was very important to get an effective work process. Errors that were discovered late in the work process could lead to a lot of lost time. With the hypothetical analysis done in Mohr-Coulomb and the case study of Gothenburg clay done in NGI-ADP, the total amount of models presented in the result reached 22.

7 Results

In this section, the results from the hypothetical case and the real case are presented.

7.1 Hypothetical case

In this section, the results from the hypothetical case, including the analytical analysis and the PLAXIS analysis with Mohr-Coulomb, are presented.

7.1.1 Analytical results

The resulting ultimate bearing capacity obtained for varying thicknesses of fill with the analytical analysis is presented in Table 13:

Table 13: Analytical result of bearing capacity

Fill height [m]	d/w_{ef}	Analytical formula	Undrained shear strength, c_u [kPa]	Bearing capacity, q_f [kPa]
0	0	$q_f=N_c c_u \xi_c$	10	51.42
0.3	0.33	$q_f=N_c^* c_u \xi_c$	10	48.89
0.6	0.67	$q_f=N_c^* c_u \xi_c$	10	57.78
0.9	1	$q_f=N_c^* c_u \xi_c$	10	66.67
1.1	1.22	$q_f=N_c^* c_u \xi_c$	10	72.59
1.35	1.5	$q_f=N_c^* c_u \xi_c$	10	80.00

The analytically calculated required fill to handle the crane load in the real case with a NGI-ADP model is presented in Table 14:

Table 14: Analytical result of required fill height for the crane case

Fill height [m]	Analytical formula	Undrained shear strength, c_u [kPa]	Bearing capacity, q_f [kPa]
1.0	$q_f=N_c c_u \xi_c$	10	69.7

7.1.2 PLAXIS results (Mohr-Coulomb)

The result obtained from the PLAXIS MC analysis is presented in Table 15. Note that the plastic plate was not evaluated for all fill options since it proved to have an intermediate value between no plate and a rigid plate.

Table 15: PLAXIS MC result of bearing capacity

Fill height [m]	d/w_{ef}	q_f [kPa] No plate	q_f [kPa] Plastic plate	q_f [kPa] Rigid plate
0	0	51.5	51.7	52.1
0.3	0.33	53.7	-	53.2
0.6	0.67	57.7	-	57.5
0.9	1	63.0	63.3	63.4
1.1	1.22	73.9	-	75.0
1.35	1.5	77.9	-	81.4

The comparison between the analytical solution and the PLAXIS MC solution is presented in Figure 19:

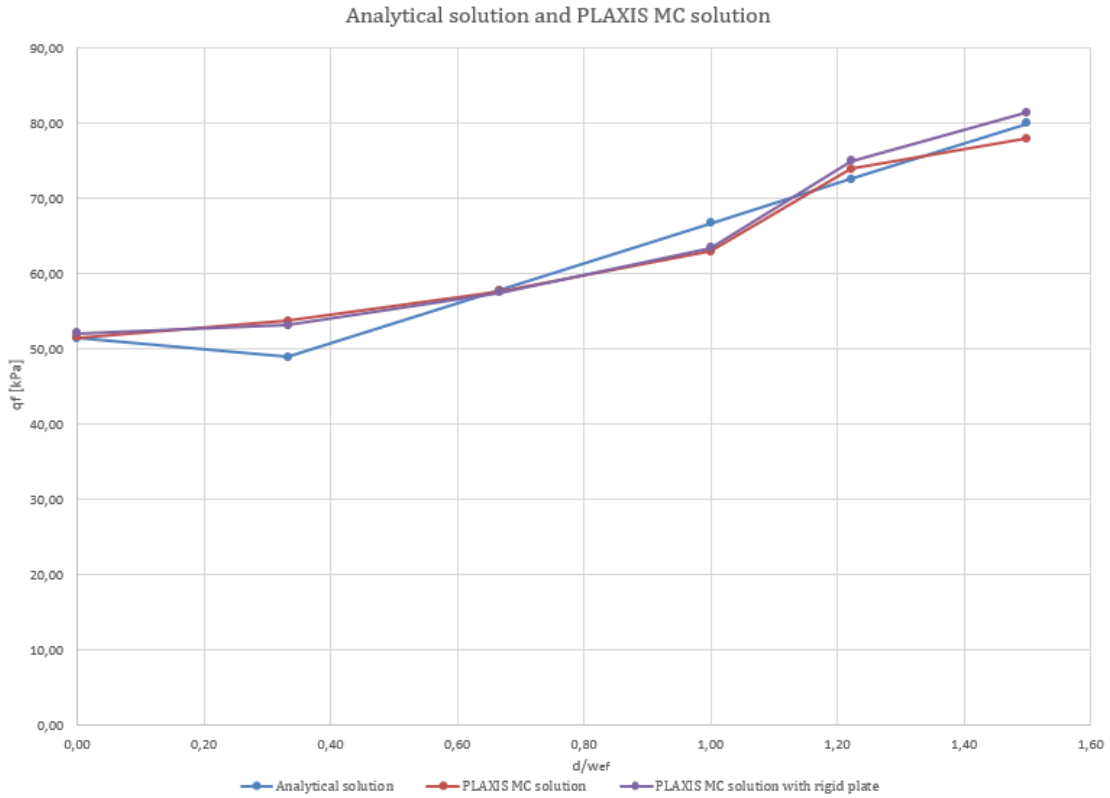

Figure 19: The analytical solution compared to the PLAXIS MC solution

7.2 Realistic case PLAXIS results (NGI-ADP)

The result obtained from the NGI-ADP analysis is presented in Table 16:

Table 16: PLAXIS NGI-ADP result of bearing capacity

q [kPa]	Tracks	$s_{u,inc}$ [kPa/m]	Anisotropy	Fill required [m]
69.7	1	0	No	1.09
69.7	1	1.5	Yes	0.89
69.7	1	1.5	No	1
69.7	1	0	Yes	0.95
69.7	2	0	No	1.09
69.7	2	1.5	Yes	0.89
69.7	2	1.5	No	1
69.7	2	0	Yes	0.9

The result shows that the minimum fill required to support the crane load are the same for both one and two tracks, with the exception of the case of only anisotropy. More required fill translates to a soil with less bearing capacity.

The result in Table 16 is presented as a bar chart in Figure 20, with a line highlighting the analytical solution:

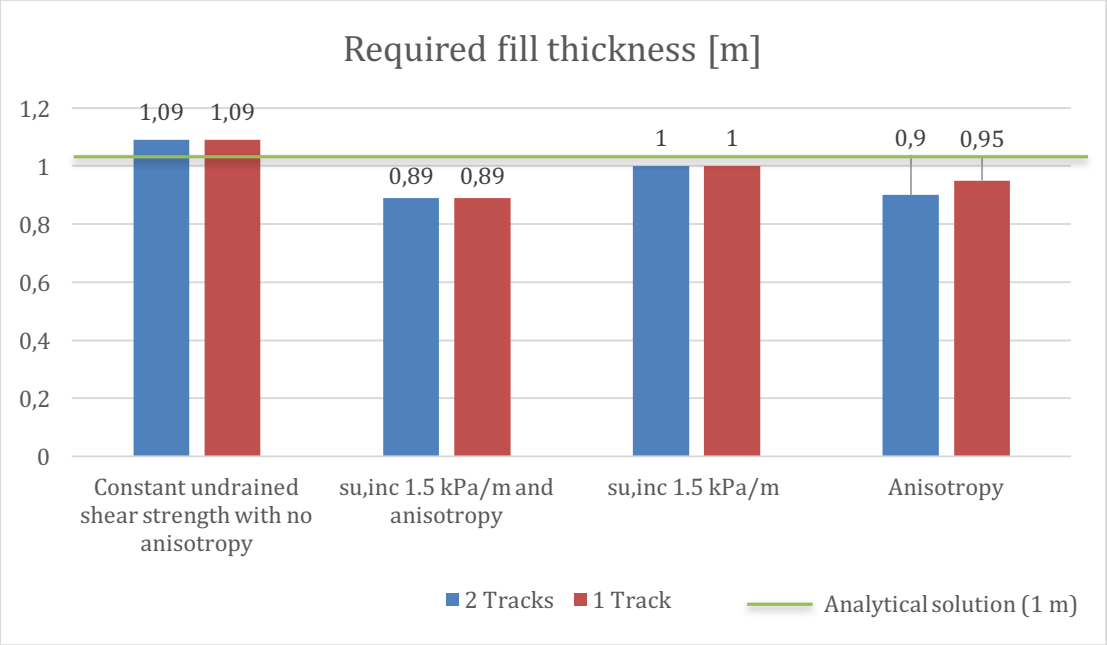

Figure 20: PLAXIS NGI-ADP and analytical result of bearing capacity

7.3 PLAXIS Plots

In this section, PLAXIS plots of the dimensionless *incremental deviatoric strain* $\Delta\gamma_s$ are presented. Plots from both the hypothetical case with a Mohr-Coulomb model and the realistic case with a NGI-ADP model are included. The $\Delta\gamma_s$ plots show the failure mechanism of each model. All the presented plots are from models where the ultimate bearing capacity has been identified, just before failure occurred. For all plots including a working platform, the interface line between the fill and the clay is highlighted and can be used as a reference depth.

7.3.1 Hypothetical case

PLAXIS plots from the Mohr-Coulomb model with a homogenous clay are presented in Figure 21, 22 and 23 for a fill thickness of 0, 0.3 and 0.6 meter respectively. The plots are presented to highlight where the shift in failure mechanism appeared.

7.3.1.1 No fill

$\Delta\gamma_s$ for no fill showed a local shear failure, down to a depth of 0.7 meter.

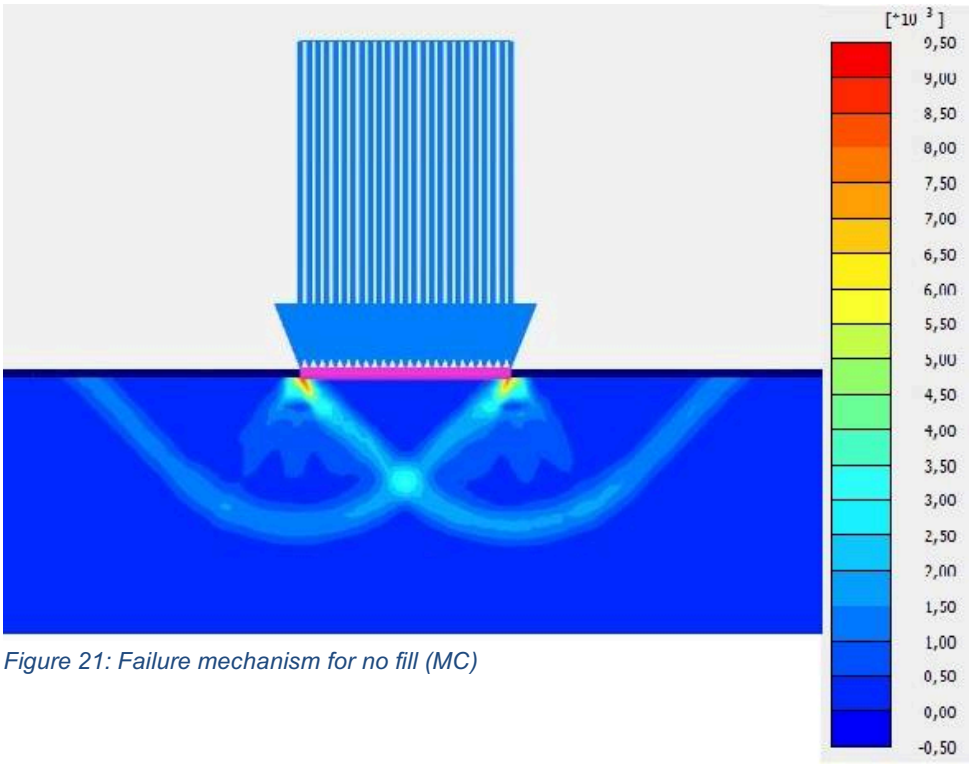

Figure 21: Failure mechanism for no fill (MC)

7.3.1.2 0.3 meter fill

$\Delta\gamma_s$ for 0.3 m fill showed a local shear failure, down to a depth of 0.5 meter below the fill.

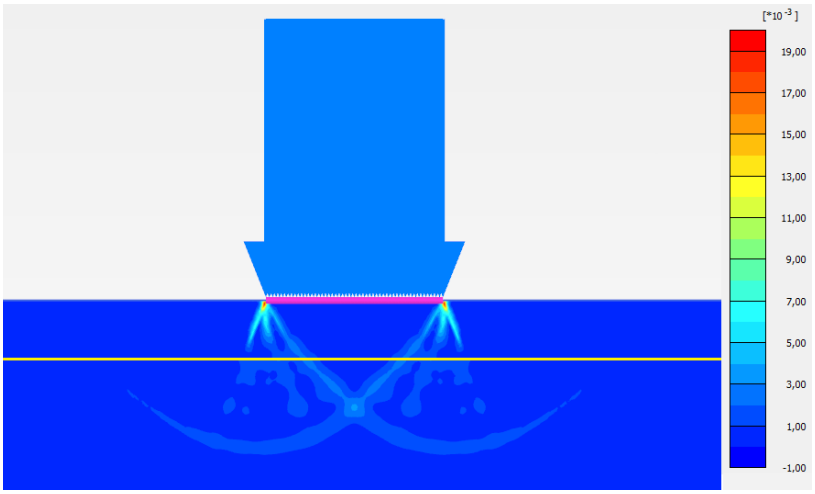

Figure 22: Failure mechanism for 0.3 meter fill (MC)

7.3.1.3 0.6 meter fill

$\Delta\gamma_s$ for 0.6 m fill showed a punching shear failure.

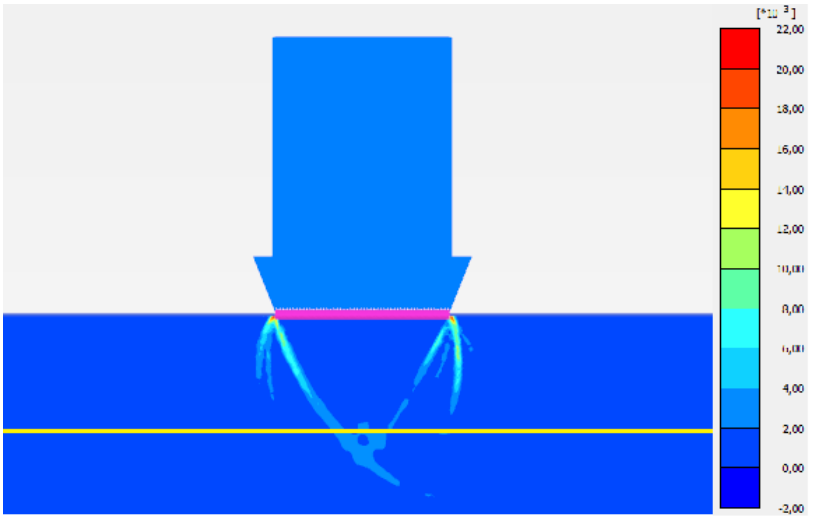

Figure 23: Failure mechanism for 0.6 meter fill (MC)

7.3.2 Realistic case

PLAXIS plots from the NGI-ADP model are presented in Figure 24-28. The four modelled scenarios are presented in the same order as for the analysis: 1) homogenous shear strength, 2) anisotropic shear strength increasing linearly with depth, 3) shear strength increasing linearly with depth and 4) anisotropic shear strength. Scenario 1 and 2 are presented for two crawlers, scenario 3 for one crawler and scenario 4 for both one and two crawlers.

7.3.2.1 Scenario 1: Homogenous shear strength

$\Delta\gamma_s$ for a homogenous shear strength showed a punching shear failure. The required fill thickness was 1.09 meter.

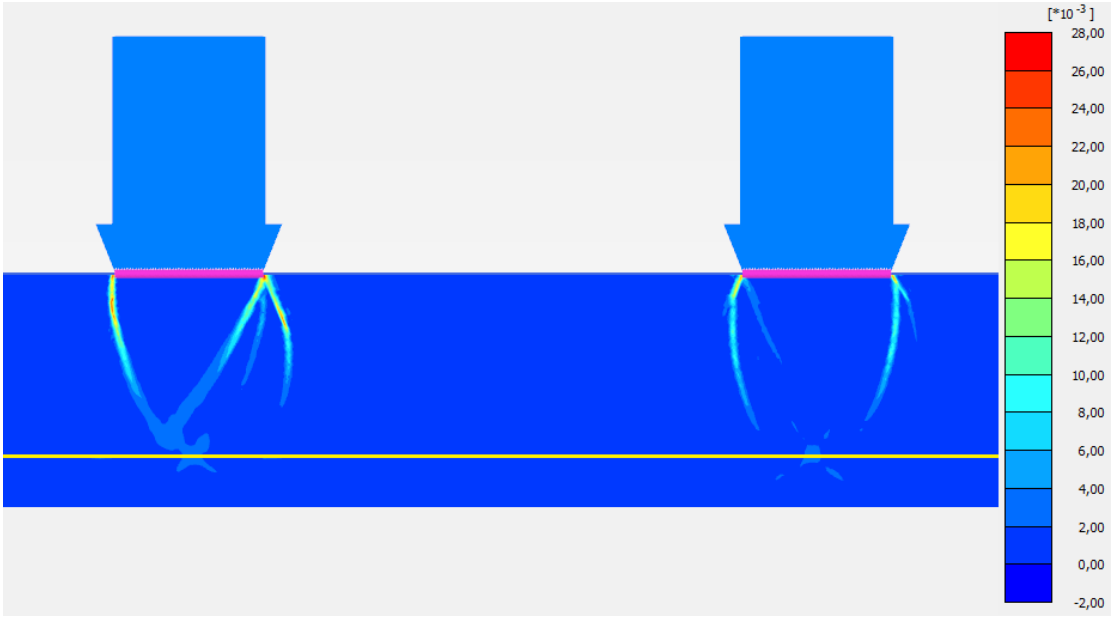

Figure 24: Failure mechanism for Scenario 1 (NGI-ADP)

7.3.2.2 Scenario 2: Anisotropic shear strength increasing linearly with depth

$\Delta\gamma_s$ for an anisotropic shear strength increasing linearly with depth showed a punching shear failure. The required fill thickness was 0.89 meter.

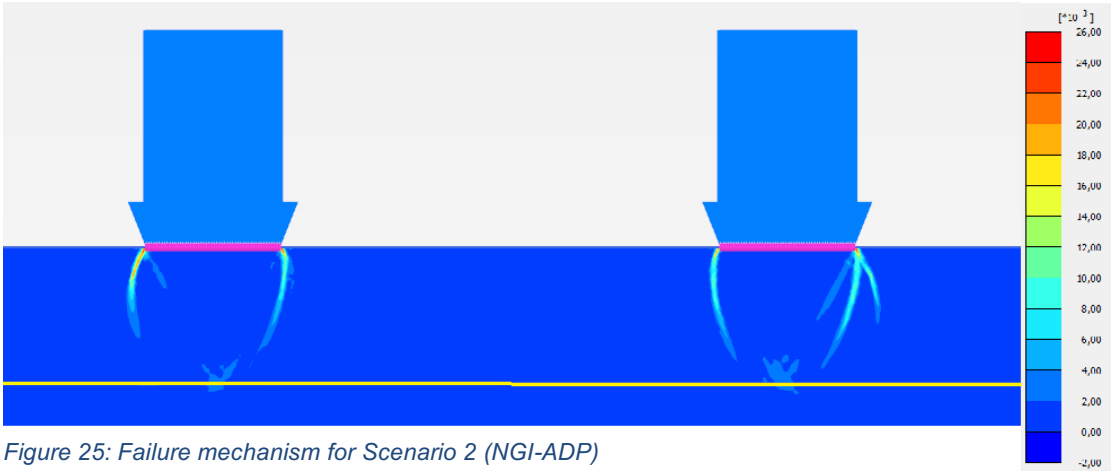

Figure 25: Failure mechanism for Scenario 2 (NGI-ADP)

7.3.2.3 Scenario 3: Shear strength increasing linearly with depth

$\Delta\gamma_s$ for a shear strength increasing linearly with depth showed a punching shear failure. The required fill thickness was 1 meter.

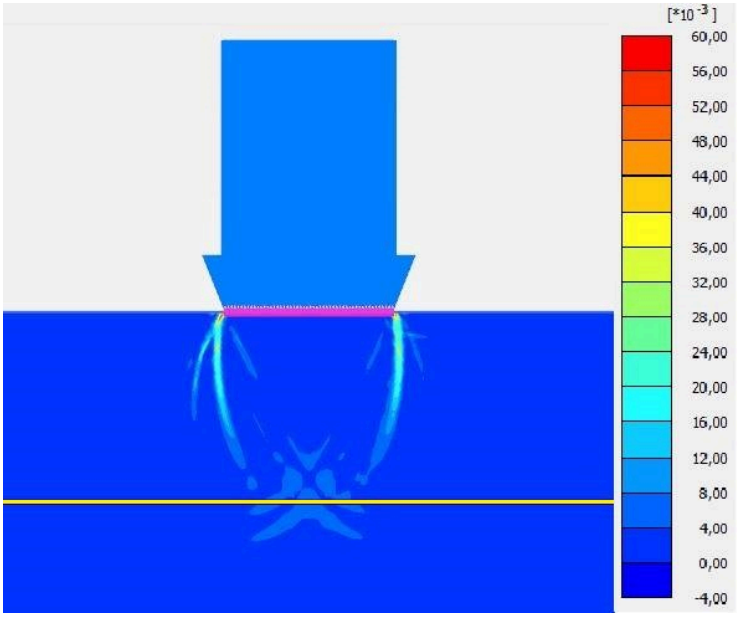

Figure 26: Failure mechanism for Scenario 3 (NGI-ADP)

7.3.2.4 Scenario 4: Anisotropic shear strength

$\Delta\gamma_s$ for an anisotropic shear strength showed a punching shear failure. The required fill thickness was 0.95 meter for one crawler and 0.9 meter for two crawlers. The possible cause for the difference in results could be that the mesh generation did not turn out completely symmetrical.

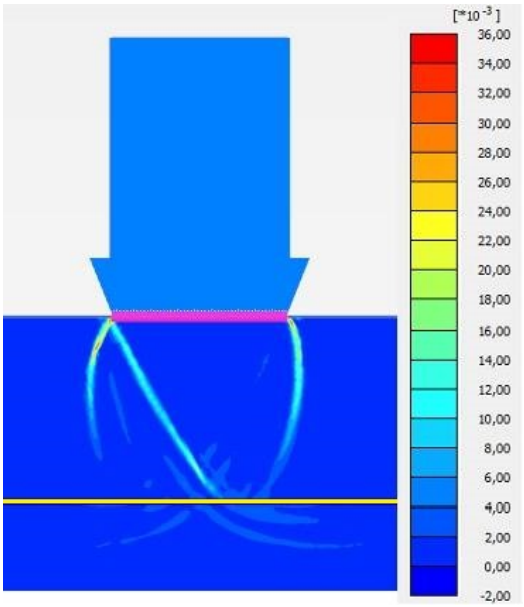

Figure 27: Failure mechanism for Scenario 4 with one crawler (NGI-ADP)

Figure 28: Failure mechanism for Scenario 4 with two crawlers (NGI-ADP)

8 Discussion

In this section follows a discussion of the hypothetical case and the realistic case, along with a numerical discussion and recommendation for further studies.

8.1 Hypothetical case

The results of the hypothetical case study show that the analytical solution is very similar to the finite-element solution for fills up to 1.35 meters. The deviation in bearing capacity is constantly low between the two analyses and the maximum difference for any fill in this range is 4.3 kPa (for 0.3 meter fill).

The output in PLAXIS showed that a local shear failure occurred for the cases of no fill and 0.3 meter fill. For fills with a thickness of 0.6 meter and above, the output instead showed a punching failure mechanism. This indicates that a switch in failure mode happens between the fill thicknesses 0.3-0.6 meters. It also indicates that the fill material did not add much additional resistance to the soil.

The PLAXIS analyses showed that fills thicker than 1.35 meters caused strikingly large settlements in the relatively soft clay due to its self-weight. This highlights another important mechanism in addition to the failure mechanism caused by the crane load; that the fill quantity has to be put in relation to the shear strength of the soil. This is something that is not accounted for in the analytical formula and therefore needs special attention. A homogenous soft clay can only support a certain amount of fill before shearing under the weight of it. As this happens, the settlements become governing over the bearing capacity in design. For this reason, the bearing capacity was not analyzed for fills thicker than 1.35 meter.

When modelling a working platform overlying soft clay, it was clear that the selection of an appropriate material model for the fill is of great importance. Using Hardening Soil Small instead of Mohr-Coulomb lead to an increase in bearing capacity of around 10 kPa. Since HS small fill overlying MC clay gave similar results as the analytical analysis, the HS small model is clearly better than the MC model for modeling fill. As a complement, it is recommended to study the recommendations in the Plaxis manual to find out which material model suits best for the evaluated geotechnical problem

The plate element used as an interface between the load and the fill had very little influence on the bearing capacity for fills up to 1 meter. An increasing influence was observed for fills larger than 1 m, where the rigid plate showed a 3.5 kPa better result for 1.35 meter fill. At this point, which marked the end of the analysis range, the analytical solution was just in between the PLAXIS solutions with a rigid plate and no plate.

The problem with thick working platforms causing settlements was briefly mentioned in IEG. However, the recommendation that a fill layer should not exceed 3-6 meter was general and not associated to any specific soil type. Therefore, the advice is hardly applicable. In this study, a homogenous clay layer with s_u 10 kPa started to experience settlement problems slightly above 1 meter of fill.

The more detailed paper presented by Hercules related soil type and shear strength to recommended fill thickness. For clay, the fill values spanned from 0.3 to 0.9 meters, which is in line with the results obtained in this study. Similar recommendations in IEG would be a great step towards more detailed guidelines regarding working platforms.

8.2 Realistic case

The starting point of this Thesis was an expectation that the general bearing capacity equation was conservative compared to finite-element solutions in the case of fill overlying soft clay. That was not the case for a simplified MC model resembling the same conditions as the formula. For the NGI-ADP model of a real case, however, the influence of shear strength anisotropy that increased with depth lead to a result where the analytical formula could be regarded as slightly conservative.

Just like in the hypothetical case with thicker fills, a punching shear failure was dimensioning for all scenarios in the realistic case. The difference between the analytical solution and the NGI-ADP solution for a homogenous clay was somewhat surprising, where the required fill for the NGI-ADP model was 9% thicker. The Mohr-Coulomb model on the other hand had a more similar result as the analytical solution. It might have to do with the different soil models used for the cases. For instance, the NGI-ADP model required input of strains. The different results caused by anisotropy for one and two tracks also stands out in the results. The explanation is most likely a numerical effect where the mesh gets different for two tracks compared to one track.

The combined effect of the implemented shear strength factors resulted in a required fill thickness of 0.9 m. That is an 18% improvement compared to the homogenous scenario in the NGI-ADP model and an 11% improvement compared to the analytical solution. After inspecting the output plots in PLAXIS, it became clear that the failure mechanism is very shallow and only a small part of the clay layer is contained in the failure mode. Hence, the results reflect the relatively small differences in shear strength for the first half meter of clay. Anisotropic shear strength increased the bearing capacity more than shear strength increasing linearly with depth; which is also explained by the shallow failure mechanism.

The modelling of two crane tracks showed little to no difference in bearing capacity results compared to one crane track. This leads to the conclusion that the crane used in the study has enough spacing between the tracks to avoid negative interactive effects when operating on soft clay. It also highlights the importance of using crane mats on soft clay; the crane load needs to be distributed over a wider area to avoid a punching shear failure.

The observation of a very shallow failure mechanism indicates that a dry crust could have significant influence on the bearing capacity of clay due to an increase in shear strength at the top of it. As already concluded, an inhomogeneous soil displays a limitation of the analytical formula. Since a dry crust is characterized by large variations in shear strength, careful soil tests are again essential in order to estimate the bearing capacity correctly.

8.3 Numerical settings

The majority of the time spent doing this Thesis consisted of model calibration in PLAXIS, as well as finding the maximum load or minimum fill for each model. During the process it was discovered that the result might vary heavily with small changes in a model. Mesh creation and numerical settings proved to have large influence on the results. It was therefore of great importance for the study that these settings were determined and motivated before running the simulations, and that the same settings applied for every model.

It should be noted that knowledge and experience of mesh creation and numerical settings is essential in order to obtain accurate results. In that sense, the results of this study are not definite and should rather be regarded as recommendations.

8.4 Further studies

The analyses performed in this study included one analytical and one finite-element method for calculating bearing capacity. Other available methods and software can be used to better understand the accuracy of the general bearing capacity equation.

The performed analyses showed how thick a working platform should be for the given soil properties in this study. Similar analyses for soils with varying properties would be of interest to approach guidelines for working platforms; where the required thickness is related to the underlying soil.

It would be interesting to analyze a similar case in Plaxis 3D, accounting for the worst load case with the carriage directed diagonally. This would include looking at overturning moment and wind load, hence getting an overview of the stability of the crane system in combination with the soil stability.

9 Conclusion

For the hypothetical cases studied, the results show that the analytical solution is similar to the finite-element solution for an isotropic soft clay. Hence, the general bearing capacity equation can be used to properly model crane foundations on working platforms overlying a homogenous soft clay.

Incorporating anisotropic shear strength or shear strength that increased linearly with depth lead to an increased bearing capacity and resulted in less required fill. Anisotropic shear strength had a larger effect than a linear increase with depth. The general bearing capacity equation can therefore be conservative if an anisotropic and nonhomogeneous shear strength profile is identified in the soil.

Simulations with a low fill thickness showed local shear failure, while thicker fills resulted in a punching shear failure. The failure mechanism, however, was very shallow and only the shear strength in the top of the clay was of importance for the bearing capacity. The shear strength and stiffness of the entire soil profile is however still of importance to account for settlements; especially for thicker working platforms.

10 References

Bergdahl, U. (1984). *Geotekniska undersökningar i fält .* Linköping: Statens geotekniska institut (SGI).

Bergdahl, U., Malmborg, B. S., & Elvin, O. (1993). *Plattgrundläggning.* Solna: Svensk Byggtjänst .

Broms, B., & Flodin, N. (1981). *Historical Development of Civil Engineering in Soft Clay .* Stockholm: Roayl Institute of Technology .

Craig, R. F., & Knappett, J. A. (2012). *CRAIG'S SOIL MECHANICS .* Milton Park: Spon Press.

Dahlgren, F., & Edstam, T. (2017). Som Man Bäddar Får Man Ligga. *Grundläggningsdagen 2017* (ss. 75-87). Stockholm: Skanska Sverige AB.

Dahlgren, F., & Nyman, V. (2015). *Working Platform on Soft Clay.* Gothenburg: Chalmers Univeristy of Technology.

Dijkstra, J. (2016). *Soil behaviour in shear .* Hämtat från Pingpong Chalmers : https://pingpong.chalmers.se/courseId/6746/node.do?id=2986703&ts=1461762753064&u=-436391696

Grahnström, A., & Jansson, O. (2016). *Estimation of collapse load on a granular working platform using limit analysis: A parametric study on a layered soil model (Master's Thesis).* Gothenburg: Chalmers University of Technology.

Hercules. (2017). Så bereder du arbetsytan för tunga maskiner. *Grundläggningsdagen 2017.* Stockholm: Hercules.

IEG. (2010). *EN 1997-1 kapitel 6 Plattgrundläggning .* Stockholm: IEG.

Junttan. (2017). Tekniska data II. (ss. 1-7). Gothenburg : Junttan .

Karlsson, M., Emdal, A., & Dijkstra, J. (den 1 12 2017). Consequences of sample disturbance when predicting long-term settlements in soft clay. *Canadian Geotechnical Journal*, 1965-1977.

Karstunen, M. (2016). *Drained and Undrained Behaviour.* Hämtat från Pingpong Chalmers: https://pingpong.chalmers.se/courseId/7001/node.do?id=3077634&ts=1467373827304&u=-436391696

Karstunen, M. (den 22 03 2016). *Geotechnical modelling III.* Hämtat från Pingpong Chalmers: https://pingpong.chalmers.se/courseId/7001/node.do?id=3077633&ts=1467373827303&u=-436391696

Larsson, R., Sällfors, G., Bengtsson, P.-E., Alén, C., Bergdahl, U., & Eriksson, L. (2007). *Skjuvhållfasthet - Utvärdering i kohesionsjord.* Linköping: Statens Geotekniska Institut (SGI).

Murthy, V. N. (2003). *Geotechnical Engineerng: Principles and Practices of Soil Mechanics and Foundation Engineering.* New York: Marcel Dekker.

Olsson, M. (2013). *On Rate-Dependency of Gothenburg Clay .* Gothenburg : Chalmers University of Technology.

Plaxis. (2017). *Company Profile*. Hämtat från Plaxis: https://www.plaxis.com/company/about-plaxis/company-profile/

Plaxis. (2017). *PLAXIS 2D Reference Manual.* Hämtat från Plaxis: https://www.plaxis.com/?plaxis_download=2D-2-Reference-1.pdf

Plaxis. (2017). *PLAXIS Material Models Manual.* Hämtat från Plaxis: https://www.plaxis.com/?plaxis_download=2D-3-Material-Models-1.pdf

Sloan, S. (2013). Geotechnical stability analysis. *Geotechnique 63*, 531-572.

Yang, X.-L., & Du, D.-C. (2016). Upper bound analysis for bearing capacity of nonhomogeneous and anisotropic clay foundation. *KSCE Journal of Civil Engineering*, 9.

Appendix

A Clay data derived from Utby soil tests

G_{ur} was obtained from a CAUC test at -6 m which is presented in Figure A1 (Karlsson, Emdal, & Dijkstra, 2017). An empirical relation was used to translate E_{ur} to G_{ur} after consulting with experts at Chalmers and ELU. The CAUC test at -6 m was also used to obtain γ_f^C. As mentioned earlier in the thesis, the STII test data is used and not the block test data.

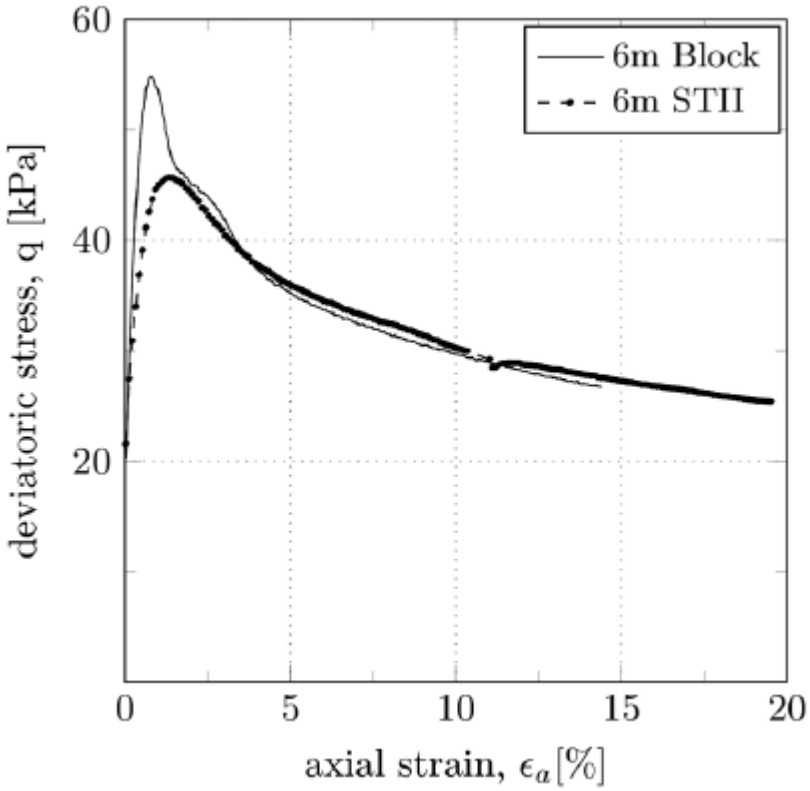

Figure A1: CAUC at -6m (Karlsson, Emdal, & Dijkstra, 2017)

$$\gamma_f^C = 1.33\ \%$$

$$E_u = \frac{\sigma}{\varepsilon} = \frac{\Delta q}{\Delta \varepsilon_a} = \frac{45.5 - 21.67\ kPa}{0.0133 - 0} = 1792\ kPa$$

$$E_{ur} = 2E_u = 2 * 1792 = 3584\ kPa$$

$$G_{ur} = \frac{E_{ur}}{2(1 + \nu_{ur})} = \frac{3584}{2(1 + 0.2)} = 1493.3\ kPa$$

A CAUE test at -7 m, which is presented in Figure A2, was used to obtain γ_f^E (Karlsson, Emdal, & Dijkstra, 2017). Even though the CAUC and CAUE tests were performed at different depths, the strain values were considered fair to use together because the close proximity of 1 m and the absence of available translation formulas. The value of γ_f^{DSS} was set to the average value of γ_f^C and γ_f^E. The value for s_u^P was also obtained from the CAUE test at -7 m. However, this value could be corrected to represent -6 m due to the assumed $s_{u,inc}$ of 1.5 kPa/m.

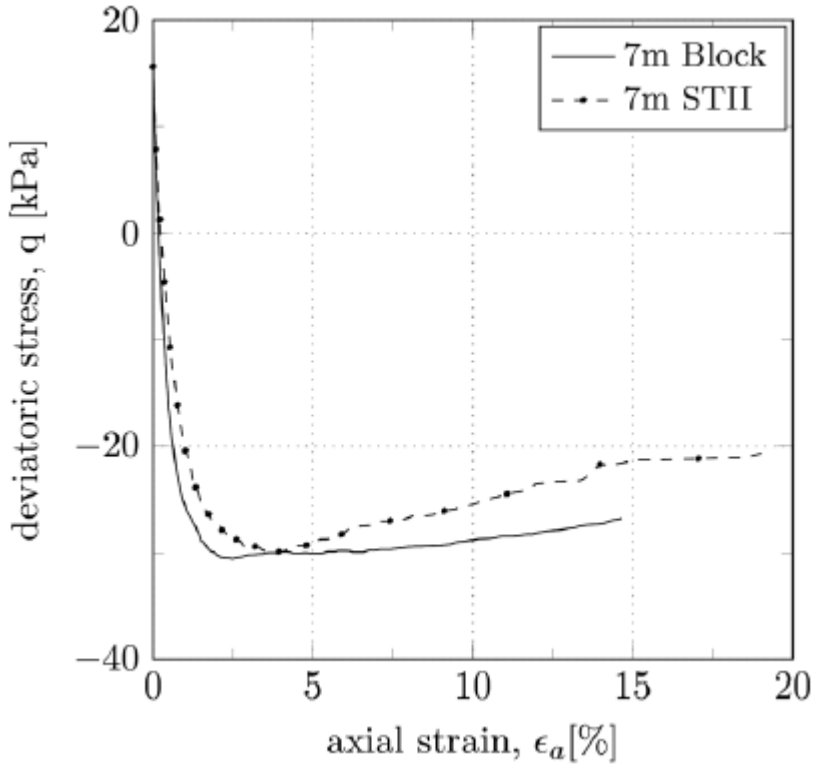

Figure A2: CAUE at -7m (Karlsson, Emdal, & Dijkstra, 2017)

$$\gamma_f^E = 3.68\ \%$$

$$\gamma_f^{DSS} = \frac{\gamma_f^C + \gamma_f^E}{2} = \frac{1.33 + 3.68}{2} = 2.505\ \%$$

$$s_u^P(-7\ m) = 30\ kPa$$

$$s_u^P(-6\ m) = 30 - 1.5 * 1 = 28.5\ kPa$$